Journal of Theoretical Biology 530 (2021) 110871

Contents lists available at ScienceDirect

Journal of Theoretical Biology

journal homepage: www.elsevier.com/locate/yjtbi

Analysis of aerodynamic and electrostatic sensing in mechanoreceptor arthropod hairs

Ryan A Palmer [a,b,*], Isaac V Chenchiah [b], Daniel Robert [a]

[a] School of Biological Sciences, University of Bristol, Life Sciences Building, 24 Tyndall Avenue, Bristol BS8 1TQ, United Kingdom
[b] School of Mathematics, University of Bristol, Fry Building, Woodland Road, Bristol BS8 1UG, United Kingdom

ARTICLE INFO

Article history:
Received 8 March 2021
Revised 29 June 2021
Accepted 11 August 2021
Available online 16 August 2021

Keywords:
Mechanoreceptor
Electroreceptor
Air flow
Electrostatics
Sensory hairs

ABSTRACT

We study the mechanics of mechanoreceptor hairs in response to electro- and acousto-stimuli to expand the theory of tuning within filiform mechano-sensory systems and show the physical, biological and parametric feasibility of electroreception in comparison to aerodynamic sensing. We begin by analysing two well-known mechanosensory systems, the MeD1 spider trichobothria and the cricket cercal hair, offering a systematic appraisal of the physics of mechanosensory hair motion. Then we explore the biologically relevant parameter space of mechanoreceptor hairs by varying each oscillator parameter, thereby extending the theory to general arthropods. In doing so, we readily identify combinations of parameters for which a hair shows an enhanced or distinct response to either electric or aerodynamic stimuli. Overall, we find distinct behaviours in the two systems with novel insight provided through the parameter-space analysis. We show how the parameter space and balance of parameters therein of the resonant spider system are organised to produce a highly tuneable hair system through variation of hair length, whilst the broader parameter space of the non-resonant cricket system responds equally to a wider range of driving frequencies with increased capacity for high temporal resolution. From our analysis, we hypothesise the existence of two distinct types of mechanoreceptive system: the general system where hairs of all lengths are poised to detect both electro- and acousto- stimuli, and a stimuli-specific system where the sensitivity and specificity of the hairs to the different stimuli changes with length.

1. Introduction

Background. In arthropods, mechanoreception using fine, light and deflectable hairs is a particularly important sensory process. This sensory modality is quite versatile, supporting hearing, fluid flow sensing, and proprioception, for a comprehensive review see Casas and Dangles, 2010. It is widespread across Arthropoda, most notably amongst insects, arachnids and crustaceans. Mechanoreceptive hairs exhibit an impressive morphological diversity, an indication of the presence of several distinct functional properties and sharp adaptations to particular sensory and non-sensory tasks. For example, a dense covering of fine bifurcate hairs can serve as thermal insulation (Southwick, 1985; Southwick and Heldmaier, 1987). It has also been noted that pollinator species tend to display hair coverings, notably with verticillate and multifurcate morphologies that facilitate pollen grain capture (Amador et al., 2017; Clarke et al., 2017).

Insects and spiders typically possess mechanosensory filiform hairs that are adapted to respond to acoustic cues and fluid flow, a sensory process that has been amply investigated and characterised (Tautz and Markl, 1978; Tautz, 1979; Shimozawa et al., 1998; Kumagai et al., 1998b; Barth and Holler, 1999a; Bathellier et al., 2005; Taylor, 2005; Humphrey and Barth, 2007; Cummins et al., 2007; Casas et al., 2008; Steinmann and Casas, 2017; Koh and Robert, 2020). The mechanosensory response of hairs and antennae has been characterised, by numerous numerical modelling and empirical studies, providing detailed knowledge of the response to fluid flow and acoustic stimuli, for key examples see Tautz and Markl, 1978; Barth and Holler, 1999a; Bathellier et al., 2005; Humphrey and Barth, 2007; Cummins et al., 2007; Koh and Robert, 2020. In some studies, particular diligence was paid to integrating the ecological and physical relevance of the stimuli considered (Casas et al., 2008; Steinmann and Casas, 2017), placing the sensor in its adequate physical ecological context (Casas and Dangles, 2010).

Only recently, however, has the capacity of filiform hairs to respond to ecologically relevant weak electric fields been unveiled in bumblebees (Sutton et al., 2016) and spiders (Morley and

* Corresponding author at: School of Biological Sciences, University of Bristol, Life Sciences Building, 24 Tyndall Avenue, Bristol, BS8 1TQ, United Kingdom.
E-mail address: ryan.palmer@bristol.ac.uk (R.A Palmer).

https://doi.org/10.1016/j.jtbi.2021.110871
0022-5193/

Robert, 2018). In nature, insects can become electrically charged through their interactions with their surrounding environment and will thus be exposed to electric fields owing to their interaction with other charged objects. As an example, these biological electrostatic interactions have been studied in bees and their interactions with floral electric fields and electric global atmospheric potential gradients (Clarke et al., 2013; Clarke et al., 2017; Koh and Robert, 2020).

Compared to fluid flow sensing, little is known yet about electrical sensitivity as a form of electromechanical sensing (Sutton et al., 2016). Notably, fluid flow sensitivity and electro sensitivity have been suggested to be equivalent with respect to the energy input required for a mechanical response (Koh and Robert, 2020). However, many questions remain regarding the underlying mechanisms enabling electromechanical actuation of bumblebee (*Bombus terrestris*) hairs. Because filiform hairs are so ubiquitous in arthropods, the prospect exists that both aquatic and aerial electroreception may be a widespread sensory modality in this Phylum. Furthermore, since electric and acoustic fields are ubiquitous in nature, there are important outstanding questions around the parametric feasibility and thus possible bimodality of electrically charged filiform hairs. One key question is how these mechanosensors that have a single morphological architecture sense both aerodynamic and electric information given the effect of their physical constraints on their sensitivity to both stimuli, with a potential trade-off in sensitivity between the two modalities.

Main contributions. In this paper we make a significant step towards answering such questions as we unveil the interplay and balance within the parameter space and geometric constraints of such hairs that together govern overall sensory mechanics. Through several novel parameter-space analyses, we show why hairs of different arthropod species, initially with specific reference to spiders and field crickets, and later to general arthropod systems, differ dramatically in their ability to be acoustically tuned and therefore in their response to aerodynamic and electrostatic stimuli. Furthermore we uncover the inherent bimodality of these hairs that results from the dependence of both sensory modalities on a shared parameter space. This is particularly significant because little research has been carried out into the effect of electric fields on these systems.

To this end, the present study (i) presents a mathematical analytical treatment of mechanosensory systems under acoustic and electric stimuli; and (ii) compares and contrasts electro- and acousto-mechanics, unveiling the key characteristics of each modality and the possible parametric interplay that governs the hair response to each modality.

The analysis presented here entails five aims: 1) to expand the theory and understanding of filiform mechanosensory systems by studying the induced torque and deflection mechanics of individual hairs under external aerodynamic and electric stimuli, 2) to understand the effect of hair tuning and oscillator parameters on the mechanics of the hair response, 3) to show the physical and biological feasibility of electroreception in comparison to aerodynamic sensing, 4) to explore the biologically relevant parameter space of mechanoreceptor hairs, 5) to identify circumstances in which a hair preferably responds to or distinguishes between electric or aerodynamic stimuli.

Moreover, we expand the parameterisation of the oscillator parameters (listed below) beyond that used in Koh and Robert, 2020. This allows for an examination of hair responses defined more generally and exploring a more widely relevant parameter space. Furthermore, expanding the parameter space through changes in each of the oscillator parameters provides a complementary and contrasting view of the mechanical response to each stimulus within a general and feasible parameter space. Consequently, we discover regions in the parameter space where there is parametric competition for sensory proficiency. Accordingly, we present a phase plane analysis that enables a visualisation of the parameter space, highlighting the wider sensory implications of variations in oscillator parameters.

Finally, we focus on the biologically-critical question of the possible dual use, or bimodality, of filiform hairs, potentially sensing both aerodynamic and electric information using a single morphological architecture. Thus, we aim to unveil the parametric feasibility of both senses within known parameter spaces, proposing a generalisation of the process to the phylum Arthropoda. Whilst the precise interplay and bimodal effect on hairs to both stimuli simultaneously is not in the immediate purpose of the present study, we will seek to extend the current understanding of mechanosensors by assessing how combinations of oscillator parameters produce contrasting or complementary responses to aerodynamic and electric stimuli.

Overview. The motion of a mechanosensory hair is generally considered to follow that of a linear, inverted pendulum with the hair acting as rigid rod (Kumagai et al., 1998b; Shimozawa et al., 1998; Humphrey and Barth, 2007). From the aerodynamic sensory viewpoint, the hair motion is tuned to different flow frequencies through the hair length L, the geometry of the hair, and the cuticular properties as described by the oscillator parameters, S, the restoring/spring constant, R, the torsional resistance/ damping constant, and I, the inertial parameter (Humphrey and Barth, 2007).

We compare the mechanical response of a hair in oscillatory fluid flows to that of a uniformly charged hair interacting with a static electric field E. Whilst it is expected that electric fields are heterogeneous in an environment containing charged flowers and insects, in studying the simpler case of a homogeneous local field, we can gain a better understanding of how the oscillator parameters influence hair mechanics. Furthermore, the use of static electric fields is reasonable due to our assumption that the evolution of the dynamic system will generally be quasi-static given the length and time scales involved.

In varying the values of L, S, R and I we will examine whether there are particular regions in the parameter space where the hair's sensitivity to electrostatic sensing increases in comparison with a range of aerodynamic stimuli, as measured by larger torques or hair deflections within an electric field. By comparing the behaviour of the mechanosensory hairs in response to the two stimuli a better understanding can be gained of the feasibility of electrical sensing in these systems, and how these systems may be biologically and physically tuned to produce an enhanced or different response for different sensory stimuli (c.f. Koh and Robert, 2020).

Given that these parameters are unknown in general, we begin our analysis by comparing the behaviour of two systems for which the oscillatory parameters are known, namely, cricket cercal hairs (Shimozawa et al., 1998, Cummins et al., 2007) and MeD1 spider trichobothria (Humphrey and Barth, 2007). We use oscillating flows of various biologically relevant frequencies and find the conditions under which equivalent hair responses are achieved under electrostatic stimuli. The metrics used to evaluate the hair responses are the maximum torque applied to the hair and the maximum angular deflection of the hair.

Another difficulty in comparing electrostatics and aerodynamics is that little is currently known about the specific parameters of electrosensory systems. To compare the two stimuli, we assume that the effect of the electrostatics on the hair is of a similar magnitude to that of the aerodynamic stimulus and thus determine the electric properties required for this to happen. This is justified by empirical evidence which shows that deflection magnitudes to aerodynamic and electric stimuli lie in the same range (Sutton et al., 2016; Morley and Robert, 2018). To evaluate the electrostatic properties of the hairs further we calculate the hair charge and

electric field magnitude required to produce a given torque or deflection angle and see how this varies with hair length and the oscillator parameters.

After such initial analyses and comparisons are made, we set out to deviate from these given values of S, R and I to examine the mechanical, sensory and biological implications using phase diagrams. We will assess how different combinations of parameters change the behaviour, tuning and mechanical response of the hairs, exploring some salient features of the parameter space. This will help us develop a more general understanding of the mechanics of these systems and the delicate interplay between the hair's physical properties and oscillator parameters within the aerodynamic and electrostatic regimes. This exploration is pertinent in view of the biological diversity of cuticular hairs, and their potential specific adaptations to specific sensory and non-sensory tasks. Importantly, we will understand how hair physical properties influence tuning and sensitivity to different stimuli.

The present analysis is not exhaustive; it constitutes a basis for future exploration of more complex scenarios. Future work will aim to develop a broader understanding of aerodynamic and electric receptors, with increased fidelity to the physical and biological properties of these systems. This includes studies of multiple hairs, different substrate geometries and electric fields; spatial and temporal effects; scales and variations in the dynamics of sound transmission and electric reception, the effects of multiple sources, or indeed different types of sound or electric sources, the complexities of hair charging and different hair charge distributions, and the biological implications of electroreception as a modality adapted to the acquisition of electric information.

Organisation of the paper. Section 2 sets out the initial modelling setup and assumptions (Section 2.1), and the methods used to model the response of mechanosensory hairs under electrostatic forces (Section 2.2) and aerodynamic forces (Section 2.3). Crucial background information is summarised in Section 3: Section 3.1 details the basic properties of harmonic oscillators and Section 3.2 applies this to mechanoreceptor hairs; Section 3.3 shows the initial analysis of the two biological hair systems comparing their responses to the two sensory modalities; and Section 3.4 discusses the variation of electrical sensitivity in the two systems as hair length varies. Building upon this analysis, Section 4 explores the wider parameter space of mechanoreceptor systems by considering the influence of each oscillator parameters on the hair response, sensitivity and tuning to each sensory modality. Section 4.1 focuses on effect of the inertial parameter through changing the hair diameter on the system, whilst Sections 4.2 and 4.3 consider the effect of the restoring parameter, and Sections 4.4 and 4.5 likewise consider the effect of the damping parameter. Then, having extensively examined the wider parameter space, Section 5 discusses the feasibility of bimodality in these biological hair systems (Section 5.1) and the implications of a single parameter determining the tuning and sensitivity of a hair to the two modalities (Section 5.2). Further considerations are made in Section 5.3 with particular attention paid to the effect of temporal dynamics on bimodality. Finally, Section 6 provides extensive discussion of the results, and conclusions on bimodality in biological systems given the single parameter space and physical properties of mechanoreceptor hairs.

2. Methods

2.1. Problem set-up

A single hair is attached to a surface that is representative of an arthropod's body, or a part thereof. The body is modelled as a bi-infinite cylinder, though an arbitrary geometry may be considered provided that the fluid flow around it is calculable. Each hair is discretised into a collection of $i = 1, \dots, n$ equidistant points, denoted x_i, that are of fixed locations along each hair. Each point is configured such that: $|x_i - x_{i-1}| = s$, for all $i = 1, \dots, n$ with $r_i = |x_i| = s \times i$ giving the length along the hair to the i-th point.

The hair acts as a rigid cylinder that is articulated at its base, where it meets the body surface, enabling it to pivot in response to external forces. The local co-ordinate system is as in Fig. 1. The hair motion is modelled as a linear, inverted pendulum and is described by the angle θ it makes with its resting position. Therefore, the motion is governed by the torque with which the hair resists the fluid motion, as follows:

$$-\tau = I\ddot{\theta}(t) + R\dot{\theta}(t) + S\theta(t), \tag{1}$$

Here, $-\tau = r \times F$ is the torque induced by the external aerodynamic force, F, acting at a distance r along the hair (hence, only the component of the force perpendicular to the hair contributes to the hair's motion). I is the inertial parameter, R is the torsional resistance/damping constant and S is the restoring/spring constant. Whilst I depends on the geometry and density of the hair, S and R are given by the properties of the viscoelastic socket membrane (Thurm, 1965a,b). The choice of these parameters are key in determining the hair's response and forms the basis of our analysis. Initially we compare cricket cercal hairs (Shimozawa et al., 1998, Cummins et al., 2007) with MeD1 spider trichobothria (Humphrey and Barth, 2007). The relevant parameters for these two systems are presented in Table 1. The definition of I in Table 1 comes from the discretisation of the cylindrical hair into n mass points $m_i = \pi\rho_h d(x_i - x_{i-1})$ for $i = 1, \dots, n$, where $\rho_h = 1100 kgm^{-3}$ is the hair density of both hair types, at each location x_i along the hair. This is valid since for $d \ll L$ the summation of the discretised I tends to the analytical definition of inertia for a cylinder. Notably there is a clear difference in the parameterisation of the two hairs with the cricket cercal hair having a value of S that is almost twice that of the MeD1 spider trichobothria, and a value of R that is nearly an order of magnitude larger for the longest hairs, $L = 1.5\ mm$.

2.2. Electrostatic modelling

For electrostatic forcing, we consider only the long-run steady state behaviour of the system. This simplifies Eq. (1) to:

$$-\tau = S\theta(t). \tag{2}$$

Here, the force that generates τ is given by the interaction of the charged hair and the external electric field. Since the hair is treated as a collection of discretised points, the hair motion is induced by the electrostatic forcing at each point along the hair.

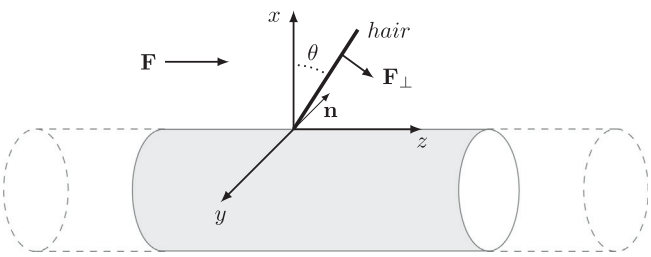

Fig. 1. The local co-ordinate system for the hair-surface system. The hair motion is on a plane with normal **n** along the y-direction. θ is the deflection of the hair from its vertical resting position in the $x - z$ plane. The component of an external force **F** that acts perpendicular to the hair, $\mathbf{F}_\perp$, induces a rotational torque τ about the hair base.

Table 1
Table of oscillator and hair geometry parameter correlations for cricket cercal hairs or MeD1 spider trichobothria. L is the hair length in metres. The allometric parameters for the cricket cercal hairs have been rearranged from their published form (Shimozawa et al., 1998) to be consistent with those of the MeD1 spider trichobothria.

Parameter	**Cricket cercal hair** (Shimozawa et al., 1998)	**Spider MeD1 trichobothria** (Humphrey and Barth, 2007)
Diameter, d m	$8.34 \times 10^{-4} L^{0.67}$	$6.343 \times 10^{-5} L^{0.3063}$
Restoring/Spring constant, S $kgm^2 s^{-2}$	$1.944 \times 10^{-6} L^{1.67}$	$1.272 \times 10^{-5} L^{2.030}$
Torsional resistance/Damping constant, R $kgm^2 s^{-1}$	$5.88 \times 10^{-6} L^{2.77}$	$2.031 \times 10^{-9} L^{1.909}$
Inertial parameter, I kgm^2	$\sum_{j=1}^{n} m_j r_j^2$	

To determine the total charge, q, of the hair it is assumed that the charge resides on the surface with a uniform density σ. The total charge is therefore dependent on the surface area of the hair and its cylindrical shape. Since the hair is slender, the charge on the end is ignored so $q = \sigma \pi d L$. Waxy surfaces endow insect cuticle with dielectric properties, exhibiting low charge mobility and therefore acting as an electric insulator (Callahan, 1975; Erickson, 1982). Assuming that the surface conductivity of the hair is low, the charge distribution is assumed to be fixed such that the charge can also be discretised at each point x_i and is given by $q_i = \sigma \pi d s, i = 1, \ldots, n$.

The arthropod is considered to be in a uniform (atmospheric) electric field of magnitude $|E|$, along $\mathbf{z}$. This is not an unreasonable assumption given the typical length scale of an arthropod (scale of millimetres to centimetres) in comparison to that of the floral electric field or atmospheric potential gradient (scale of metres to kilometres). When the discretised hair is placed in this external electric field, the Coulomb interaction produces a force at each point considered on the hair, the sum of which gives the total force over the hair. Denoting the external electric field at the i^{th} point as $\mathbf{E}_i = E(x_i)\mathbf{n}_E$, the Coulomb force exerted on the hair point is given by:

$$\mathbf{F}_i = \mathbf{F}(x_i) = E(x_i) q_i \mathbf{n}_E. \tag{3}$$

2.3. Aerodynamic modelling

The method we use to model the aerodynamic response of a hair is developed in Cummins et al., 2007; Cummins and Gedeon, 2007. This method was chosen due to the discretised representation of hairs. As such, the method is directly comparable to that of the electrostatic modelling used since the aerodynamic forces acting on the hair are also calculated for each hair point and distributed over the hair. The sum of these forces in both cases provides an accurate depiction of the hair movement. Furthermore, this method allows for flexibility in both the definition of the hair geometry, due to the discretised moment of inertia, and of the substrate that will be beneficial in future studies addressing hair diversity. In choosing the method, we compared the modelling results (not shown) with an alternative method from Humphrey and Barth, 2007 and found the results to qualitatively and quantitatively match the aerodynamic regimes considered in this study. Furthermore, some of the limitations of the method as noted in Cummins et al., 2007 to accurately model these systems were overcome using the adaption presented in Cummins and Gedeon, 2007 to ensure the physicality of the results and correct application of the boundary conditions. To this end, we applied a two-step iteration method as in Cummins and Gedeon, 2007 to calculate the perturbed boundary layer and reduce any potential errors.

A brief overview of the method is given below and we refer interested readers to the original papers for full details. This model follows a slender body assumption which is valid when the radius of the hair is significantly smaller than the length. This assumption is commonly applied in both the case of low Reynolds number fluid flow (Stokes flow) and in cases of electrostatic modelling and is therefore appropriate for the scenarios modelled below.

To model the effect of a biologically relevant aerodynamic stimulus, the fluid flow is considered to be generated by the sound of a nearby insect and thus takes the form of a sinusoidally oscillating far-field air motion. The periodic flow is therefore modelled along the cylinder for a range of biologically relevant frequencies, $f = 30 - 230$ Hz and far-field velocities $V_0 = 15 - 55\ mms^{-1}$. This range of frequencies between 30 Hz and 230 Hz has been shown to represent the wing beat of nearby insects (Tautz and Markl, 1978), whilst lower frequencies ($30 - 80\ Hz$) have been shown to constitute the adequate stimulus for cricket hairs (Shimozawa and Kanou, 1984), and form the frequency composition of ecologically relevant flows (Steinmann and Casas, 2017). Due to the bi-infinite cylinder body geometry an analytical solution exists for this fluid flow over body surface and can therefore be readily calculated to give the background flow that perturbs the hair as in Cummins et al., 2007.

A no-slip boundary condition at the body surface causes the sinusoidal flow over the cylinder to produce an oscillating Stokes boundary layer along the surface as in Humphrey et al., 1993. Notably, both the period ($T = 1/f$) and thickness of the Stokes boundary layer ($\delta = \sqrt{4\pi\nu/f}$, where ν is the kinematic viscosity of the fluid) change with frequency, as depicted in Fig. 2. The Stokes boundary layer thickness is defined as the normal distance from the surface at which the flow velocity has essentially reached the freestream velocity. To model the hair motion, a hair is placed somewhere along the cylindrical substrate and extends into this Stokes boundary layer flow.

Importantly, due to the biological and physical scales considered, the Reynolds number of the fluid flow is low such that the background flow can be calculated using steady Stokes equations. This allows for the calculation of the perturbation velocity that induces the hair motion using the method of Stokeslets (Cortez, 2001). To fully model the system, τ also consists of contributions from the no-slip boundary conditions on the hair and body surfaces, and the constraining forces that ensure the planar motion of the hair alongside the resisting force of the hairs and the force of the perturbing airflow noted above. Therefore the hair-flow coupling and overall hair motion can be modelled as in Cummins et al., 2007. and by applying the previously noted two step iteration method in Cummins and Gedeon, 2007 to reduce any potential errors.

Hair length is an important factor in the overall response and parameterisation of mechanorecpetive hairs since it is used to calculate the geometrical properties of the hair and the oscillator parameters as noted in Table 1. In considering aerodynamic sensing, it is expected that the range of biologically relevant hair lengths will fall within the range of the Stokes boundary layer depths produced by the insect sound frequencies to "guarantee that most of the hair length will experience the full amplitude of the oscillating flow" (Humphrey and Barth, 2007). Furthermore, hairs that are longer than these Stokes boundary layer thicknesses will have a diminishing return in terms of their sensory ability since the deflection angle will decrease with hair length. In addi-

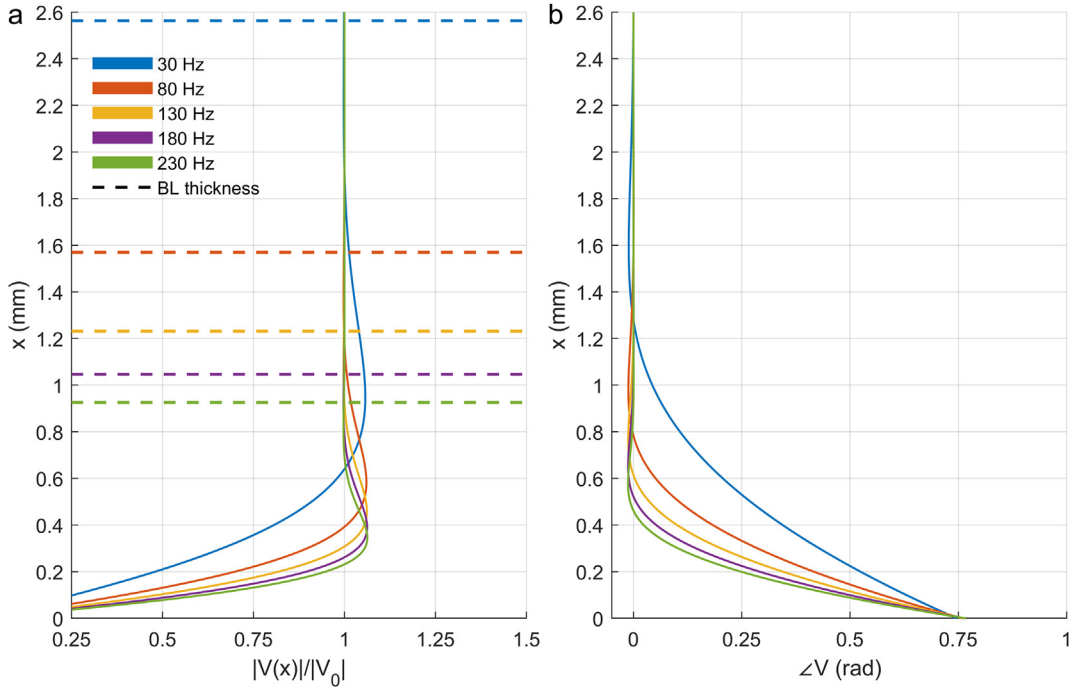

Fig. 2. For an oscillating Stokes layer along a bi-infinite cylinder with various frequencies and $V_0 = 35 mms^{-1}$, at a distance x from the surface: (a) Normalised velocity profiles and boundary layer thicknesses. (b) Phase of the fluid flow.

tion, the cuticular properties (values of S and R) and hair geometry (value of I) will change, affecting the tuning of the hairs to no longer match the frequencies it is required to detect (Humphrey and Barth, 2007).

For this reason we consider hairs of length $L = 0.25 - 1.5\ mm$ to match the Stokes boundary layer thicknesses of the biologically relevant frequencies, as analysed in this paper and shown in Fig. 2. Here, the far-field flow speed is $V_0 = 35\ mms^{-1}$ since this is in the middle of the suggested $15 - 55\ mms^{-1}$ range (Tautz and Markl, 1978). Notably, for the 30Hz and 80 Hz flows the Stokes boundary layer thickness covers all hair lengths, whilst the 230 Hz flow has the smallest thickness, under 1 mm.

3. Initial analysis

In this section, we first remind the reader of the key theory and characteristics of harmonic oscillators (Section 3.1). We then highlight parametric differences between cricket cercal hairs and MeD1 spider trichobothria, considered as harmonic oscillators (Section 3.2). While this information is already found in the literature, it is summarised here for the convenience of the reader since it is crucial to the subsequent analyses and discussions. Finally, we examine the consequent differences in the aerodynamic (Section 3.3) and electrostatic responses (Section 3.4) of these hair types.

3.1. Harmonic effect of the oscillator parameters

Damping and resonance. Each oscillator parameter has a distinct influence on the motion of the system: The restoring coefficient S determines the magnitude of the force that acts to bring the hair back to its equilibrium position; the damping coefficient R determines the magnitude of the frictional force that opposes the hair motion due to viscous drag and friction in the system; and the inertia coefficient I determines the magnitude of the force that opposes the acceleration of the hair. Together, these parameters determine the qualitative oscillatory behaviour of the hair system as governed by the damping ratio (French, 2003; Taylor, 2005),

$$\zeta = \frac{R}{2\sqrt{IS}}.$$

When $\zeta > 1$ the system is overdamped and damping is dominant in the hair response: perturbing the hair from its equilibrium position will cause it to return to equilibrium exponentially-decaying without any oscillation. The closer ζ is to 1 the faster the system returns to the steady position with the system returning most quickly when $\zeta = 1$ which is known as critical damping. This is the threshold between the non-oscillatory and oscillatory behaviour.

When $\zeta < 1$ the system becomes underdamped and the hair will oscillate when perturbed. Over time the system will return to steady state with an exponentially-decaying amplitude of oscillation. For smaller ζ the system returns to steady state more slowly and will oscillate more. In addition, when $\zeta < 1/\sqrt{2}$ the system becomes resonant such that a resonant frequency exists at which a driven oscillator has an enhanced response. This causes the amplitude of oscillation to increase and the resistance of the hair to decrease in comparison to non-resonant systems or when the driving frequency is far from the resonant value. When $1/\sqrt{2} < \zeta < 1$ we refer to the system as being slightly underdamped, whilst for $\zeta < 1/\sqrt{2}$ we refer to the system as being resonantly underdamped.

Three different frequencies determine the tuning of each hair. Firstly, the undamped natural frequency,

$$f_0 = \frac{2}{\pi}\sqrt{\frac{S}{I}},$$

is the frequency at which an undamped hair ($R = 0$) would oscillate if all other parameters are kept the same. Secondly, the underdamped natural frequency,

$$f_1 = f_0\sqrt{1-\zeta^2},$$

is the frequency at which a damped hair such that $\zeta < 1$, would oscillate if perturbed. Thirdly, the resonant frequency,

$$f_r = f_0\sqrt{1-2\zeta^2},$$

is the frequency at which the enhanced oscillator response occurs and indicates a specific tuning of the hair (only for damped hairs such that $\zeta < 1/\sqrt{2}$).

3.2. Mechanoreceptors as harmonic oscillators

Given the differences in the parameters correlations in Table 1 and the above definitions, the two hairs will have distinct harmonic properties, as shown in Fig. 3. Fig. 3(a) shows the damping ratio ζ of the two hairs as their length varies. It can be seen that the cricket hairs are initially overdamped for length $L \sim 0.25\,mm$ but soon become slightly underdamped as length increases until $L \sim 1.3\,mm$ when the hairs become resonantly underdamped. The MeD1 spider trichobothria however are resonantly underdamped for all hair lengths. Therefore, it is expected that the two types of hair will behave quite differently in response to the same aerodynamic stimulus. Indeed, the aerodynamic responses of these two have been widely studied within the literature. For examples regarding spider trichobothria see Humphrey and Barth, 2007; Humphrey et al., 1993; Barth et al., 1993; Barth et al., 1995; Barth and Holler, 1999b; Barth, 2004 and the references therein. Likewise, for examples regarding cricket cercal hairs see Shimozawa et al., 1998; Humphrey and Barth, 2007; Shimozawa and Kanou, 1984; Kumagai et al., 1998a; Landolfa and Miller, 1995; Magal et al., 2006; Jacobs, 1995; Shimozawa et al., 2003 and the references therein.

Furthermore, the difference in the oscillator parameters lead to a different tuning of the hairs as shown in Fig. 3(b), which presents the three different frequencies, noted above, for each hair type. In each case, different hair lengths have a different natural tuning, and thus different mechanical responses are expected based on the frequency of the surrounding flow.

MeD1 spider trichobothria. For the spider hairs, the undamped, underdamped and resonant frequencies are all close to one another (see Fig. 3(b)) indicating that for small ζ the hairs are resonantly tuned across the different hair lengths to the biologically relevant frequencies that are analysed here. Interestingly the hair lengths also closely match the boundary layer thicknesses for the relevant frequencies. Additionally, Fig. 3(b) shows the bandwidth for hairs that are resonantly underdamped. The bandwidth is the range of frequencies for which a driven oscillator has at least half the energy of the peak resonant value. Thus, whilst the natural/resonant frequency is less than 230 Hz for most hair lengths, there is a large bandwidth for smaller hairs such that the hair response will still be amplified for frequencies that are further from the resonant frequency.

Cricket cercal hairs. For cricket cercal hairs the dynamics and properties are very different. The system is initially overdamped with a large natural frequency far outside what is considered to be the biological range, see Fig. 3(b). As the damping ratio decreases the natural frequency falls and the underdamped natural frequency begins to exist. Overall the underdamped natural frequency is within the bounds of the biological frequencies (for $L > 0.5\,mm$), however damping within the system is still significant. For the longest hairs resonant behaviours are possible for low frequencies.

3.3. Frequency analysis of the hair motion

A single hair of each type is modelled in a range of different frequency flows (30–230 Hz) to assess the effect of the oscillator parameters and hair length on their mechanical response, see Fig. 4. In each case, the correlations in Table 1 are used to parameterise the hair models. An envelope for the electrostatic response of each hair is included in Fig. 4 to show values of $\sigma|E|Nm^{-2}$ that produce a similar hair response for the range of hair lengths.

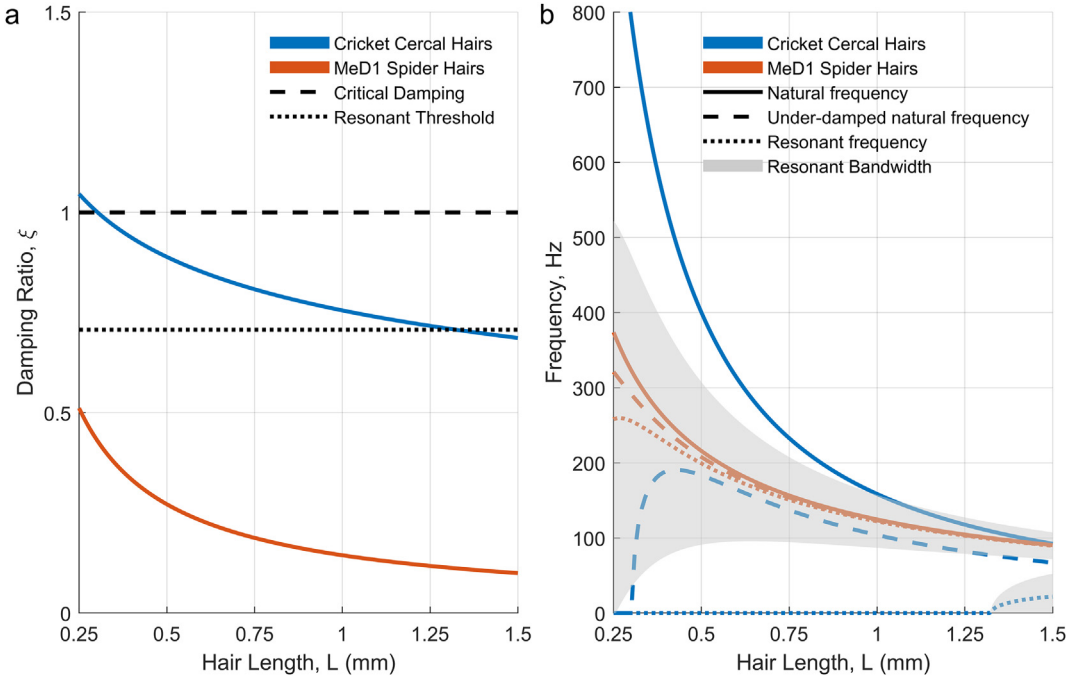

Fig. 3. (a) Damping ratio, ζ, for MeD1 spider trichobothria and cricket cercal hairs as functions of length. Dashed line indicates critical damping $\zeta = 1$, dotted line shows region of resonance $\zeta \leqslant 1/\sqrt{2}$. (b) Undamped natural frequency, underdamped natural frequency and resonant frequency of MeD1 spider trichobothria and cricket cercal hairs as functions of length. Bandwidths for the hairs in the resonant underdamped regime are shown in grey.

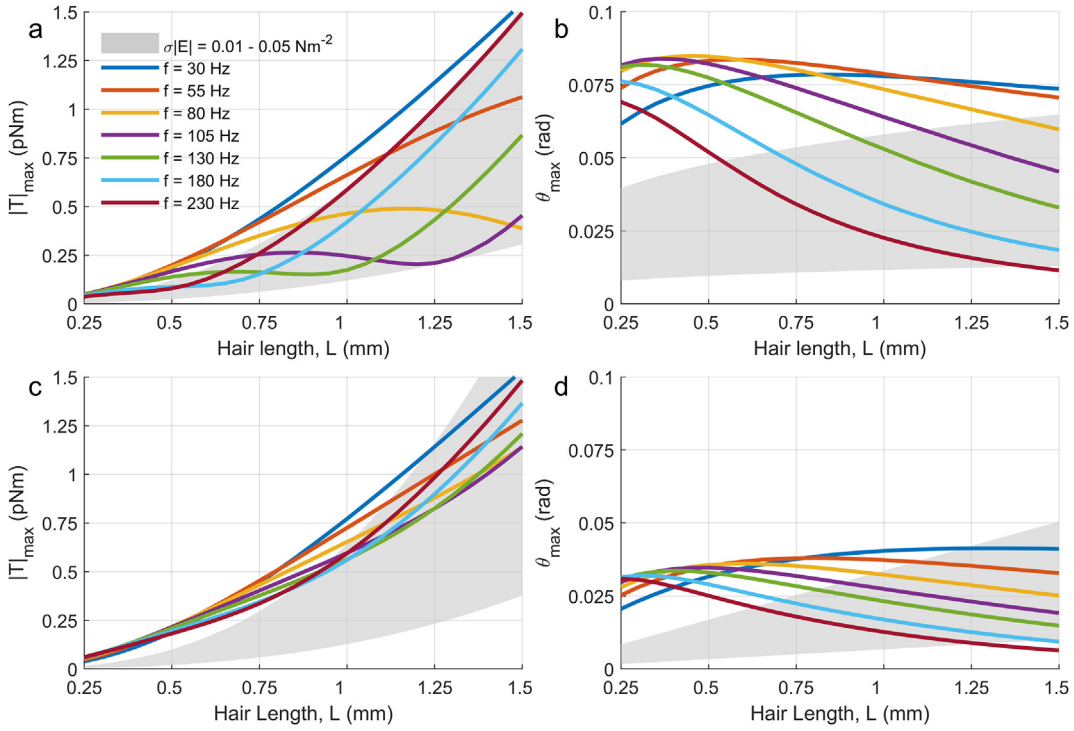

Fig. 4. Analysis of torque and hair deflection as a function of frequency (a,c) Maximum torque applied to hairs of varying lengths in different frequency flows. (b,d) Maximum deflection for hairs of varying lengths in different frequency flows. Panels (a,b) show results for MeD1 spider trichobothria and (c,d) for cricket cercal hairs. The grey envelopes indicate the range in torque response and hair deflections at each length for electric field interaction strengths $|E| \in [0.01, 0.05] Nm^{-2}$.

MeD1 spider trichobothria The response for the range of hair lengths varies significantly with frequency. There is a wide range of responses in generated torques from the monotonic relationship of the 230 Hz flow to the increasing and decreasing dynamics of the 80 Hz flow, 105 Hz flow, 130 Hz flow and 155 Hz flow responses. One reason for this is the change in the resonant tuning with length. In particular, the local minima of the torque curves for the 105 Hz, 130 Hz and 155 Hz flows in Fig. 4(a) match with the lengths in Fig. 3 where these are the hair's resonant frequency (L = 1.25 mm, 0.9 mm, 0.8 mm respectively). These minima are less distinct for the shorter hairs since the bandwidth is larger in these cases. Additionally, if we modelled hairs of length $L > 1.5\ mm$ we would find the resonant minimum in the torque response for the 80 Hz flow.

In each of the above cases resonance does not change the overall trend in hair deflection. In effect, resonance reduces the hair's resistance to a flow of a given frequency such that the angle of deflection per unit torque of the hair increases. This results in increased sensitivity. For flow frequencies far away from the resonant frequency the hair resistance greatly increases, e.g. the 230 Hz flow response has comparatively large torques and small deflections for most hair lengths.

Cricket cercal hairs The dynamics here vary less with frequency and there are narrower ranges in the torque responses, Fig. 4(c), and deflection responses, Fig. 4(d). Overall, the same trends with frequency and length, as in the spider case, are seen in the cricket case with the same ordering of torque and deflection profiles with frequency. The main difference here is the lack of resonance in the cricket hair system since it is slightly underdamped over the majority of hair lengths. Thus, the cricket hairs have a greatly diminished response to the flow and less discrimination between frequencies with length. The torque is generally larger overall, as a result of the oscillator parameters being comparatively larger and therefore causing a greater resistance to the air flow.

3.4. Electrostatic analysis of the hair motion

Regarding the electrostatic response of hairs, the electric envelopes presented in Fig. 4(a,c) cover most of the torque responses at each hair length. Notably the relationship here is purely monotonic and, under the modelling conditions, there is no analogy to the resonant effect. Regarding hair deflections, Fig. 4(b,d) shows a distinct change in the hair response. An increasing relationship between length and deflection is seen which is counter to the notion of the deflection angle decreasing with hair length under aerodynamic stimuli (Humphrey and Barth, 2007). This effect is due to the total surface charge increasing with the hair's length and diameter due to the increased surface area.

Interestingly, the values of $\sigma|E|$ shown here are smaller than those in Koh and Robert, 2020, however they are of a similar order of magnitude and are physically relevant. The response envelopes show that is it biologically and mechanically feasible for hairs to detect electric fields using the same mechanisms as in aerodynamic sensing.

In the aerodynamic case, length changes the overall response of the hair to different flows. Thus, we seek to understand how length affects the electrostatic sensitivity and response of the hair. To this end, Fig. 5(a) shows how the torque changes with length as measured by $|T|/\sigma|E|$, a measure of electromechanical sensitivity, and Fig. 5(b) shows how the hair deflection changes with length as measured by $\theta/\sigma|E|$.

The results in Fig. 5(a) show that for a fixed value of $\sigma|E|$ longer hairs undergo a larger torque in comparison to smaller hairs. This is due to both the increased total hair charge with length producing a larger Coulomb force over the hair and the increasing values of S and d. In fact, the precise scaling of torque with length can be found from the allometric parameters given in Table 1. For the spider hairs the torque scales as $L^{2.3063}$ whilst for the cricket case the torque scales as $L^{2.67}$ indicating the near-quadratic response of both

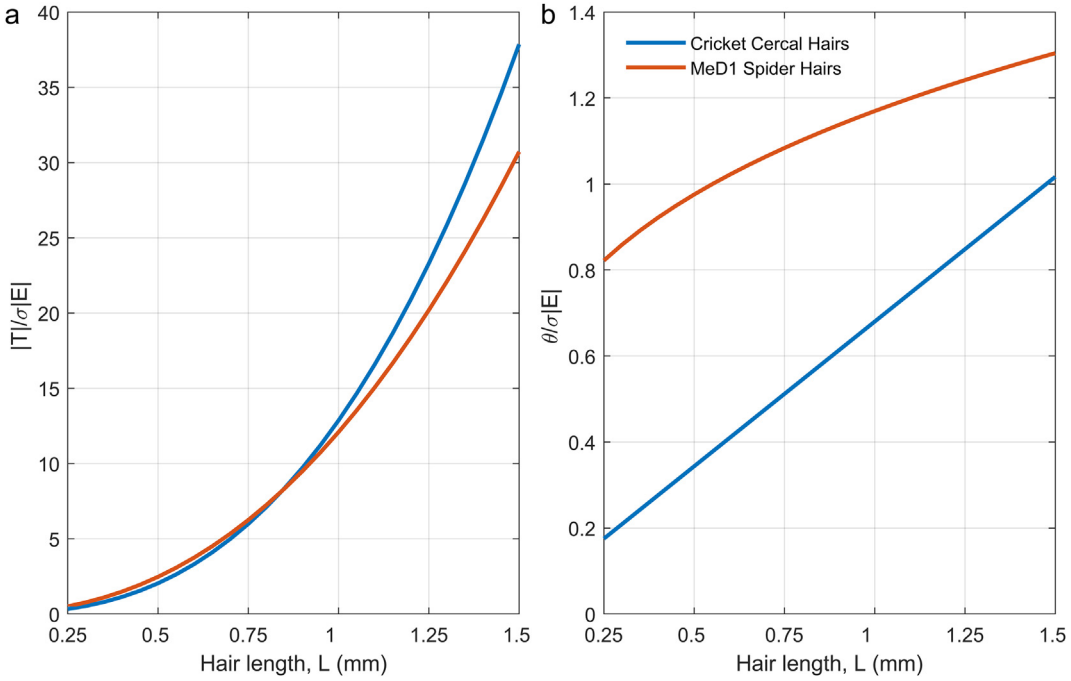

Fig. 5. For MeD1 spider trichobothria and cricket cereal hairs (a) torque per unit $\sigma|E|$ and (b) deflection per unit $\sigma|E|$, as length varies.

hairs and showing why the cricket torque profile overtakes the spider response at about 0.8 *mm*. Due to this superquadratic relationship, the difference in the hair response is greatly enhanced with length indicating a clear differentiation in the torque sensitivity of hairs with length.

Furthermore, the results in Fig. 5(b) show that for a fixed value of $\sigma|E|$ longer hairs will undergo larger deflections in comparison to smaller hairs, highlighting an increased sensitivity to electrostatic stimuli with the increased total charge due to length. One point of interest however is that whilst the overall values for the cricket cercal hairs are lower, the steeper gradient indicates a greater differentiation in electrostatic sensitivity of hairs with length. In this situation the variation in S with hair length plays a significant role. Again, the precise relationship with length can be obtained from the allometric parameters in Table 1. For the cricket hairs the scaling is exactly linear whilst for the spider hairs it scales as $L^{0.2763}$. This further explains the shape of the curves and the larger variation in the response of the cricket hairs with length.

4. Parameter-space analysis

To further analyse this system we now perturb from the given allometric parameters to explore how varying either I, S or R affects the hair's aerodynamic and electrostatic response. Having seen distinct mechanical behaviours arising from the different hair and cuticular parameters, the purpose of this analysis is to consider further the wider biological parameter space that may be relevant to other arthropods. To explore this putative generalisation, we consider variations in the parameter space that are within an order of magnitude from the spider and cricket parameters. This approach is aimed at providing an insight into possible morphological adaptations across arthropod phyla.

4.1. Hair response for varying the inertia coefficient, I

For a hair of fixed length, for I to change either the hair's diameter or the hair density must change. It is currently unclear how changing the density may affect the electrostatic response of the hair. Changing the diameter, however, will have an effect on both the hair's total charge and its aerodynamic tuning. Therefore, we will focus on this case, see Fig. 6. As before, we consider hairs of length $L = 0.25 - 1.5\,mm$ and a far-field magnitude of $V_0 = 35\,mms^{-1}$ to enable comparison with the previous results. The flow frequency is taken to be 130 Hz for all cases. Since the resonant frequency of each hair changes with length and diameter, this illustrates how the resonant tuning of hair, whether it is far from or close to 130 Hz, affects the mechanical response.

Increasing the value of I has two effects of interest on the tuning of thicker hairs. Firstly, the thicker hair experiences an increased overall torque due to a greater resistance to the flow. Secondly, the damping ratio, natural frequency and therefore the resonant frequency (where applicable) will all decrease. What is the consequent overall impact on the hair dynamics? As shown in Fig. 6, when increasing diameter and therefore I, both the MeD1 spider trichobothria and cricket cercal hairs have resonant responses at the 130 Hz frequency for hairs of $L \sim 0.35\,mm$ and $L \sim 0.5\,mm$ respectively. Decreasing the diameter, and therefore I, results in reduced magnitudes of response in both cases as the relative damping increases and the hair tuning changes.

In detail, Fig. 6(a,b) shows that the spider hairs again have a wider range of dynamic responses compared to cricket hairs, Fig. 6(c,d). For decreasing diameter, the hair spider system is still in the resonant regime for most lengths, however the resonant frequency has increased for each length such that hairs now begin to show the resonant response in the torque profiles at longer lengths (compared to Fig. 4a). Decreasing diameter for cricket hairs has very little impact on the overall behaviour since increasing damping ratio only makes the hairs more overdamped.

For thicker hairs, however, the dynamics are notably different since both hair types are now resonantly damped with resonant frequencies of around 130 Hz for the shortest hairs of both hair types ($L \sim 0.35\,mm$ for spider hairs, $L \sim 0.5\,mm$ for cricket hairs). At these small lengths resonance introduces a significant peak into the hair deflection results. This differs from the low torque resonant response seen before in Fig. 4. The bandwidth of cricket hairs

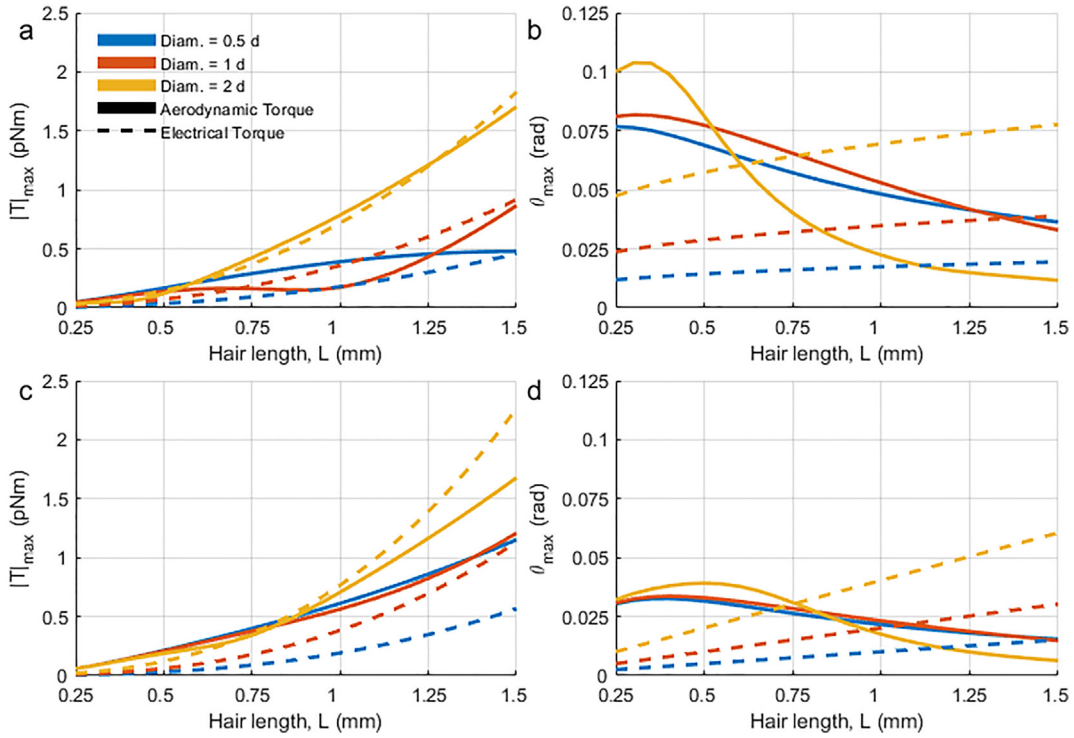

Fig. 6. (a,c) Maximum torque applied to hairs of varying lengths with different diameters in 130 Hz flow. (b,d) Maximum deflection for hairs of varying lengths with different diameters in 130 Hz flow. Panels (a,b) are the results for MeD1 spider trichobothria and (c,d) are the results for cricket cercal hairs. The dashed lines for the electrostatic interaction related to an electric field interaction of $\sigma|E| = 0.03\ Nm^{-2}$.

is much larger which is why there is less variation between short and long hairs compared to the spider hairs. Overall, these results point to hairs where the damping ratio is within the resonant range due to a large relative I having distinct deflection responses across differing hair lengths when driven at the resonant frequency. An array of such hairs would confer reliable frequency discrimination to the arthropod.

Electrostatic sensitivity. Regarding the electrostatic responses, the dashed lines in Fig. 6 are each of a similar order of magnitude to the aerodynamic responses for a value of $\sigma|E| = 0.03$. The relationship between length and both torque and hair deflection are again monotonic with the overall change in the electric response being linear with the diameter (c.f. the definition of q in Section 2.2). With regards to deflections, longer hairs again have larger deflections in spite of their length, with the thickest hairs deflecting most. Notably, the magnitude of the electric response of thinner hairs is far below or near that of the aerodynamic cases. These trends occur due to the total surface charge increasing with hair's surface area and therefore increasing with both length and diameter, as explained in detail below.

Examining the electrostatic response of different hair lengths and diameters, we now seek to understand how hair length affects the electrostatic sensitivity and response of the hair. Fig. 7(a) and (b) show how the torque per unit $\sigma|E|$ and the hair deflection per unit $\sigma|E|$, respectively, change with length and diameter.

The results closely resemble those presented in Fig. 5, with longer hairs undergoing larger torques and hair deflections in comparison to smaller hairs. The same scalings with length as found in Section 3.4 continue to hold here. Now for a fixed value of $\sigma|E|$, we also see the response of a hair scaling linearly with diameter. Thus, the difference in the hair responses reveal a clear differentiation in torque sensitivity and deflection with both length and diameter.

4.2. Hair response for varying the restoring coefficient, S

The effect of perturbing S by a multiplier $S_m \in [0.1, 10]$ is now explored through the examination of hair torques and deflections of three lengths of hair, $L = 0.5, 1.0, 1.5\ mm$. In general, increasing the value of S has two effects of interest on hair tuning. Firstly, it will decrease the damping ratio at a given length causing the resonant frequency to be set more closely to the natural frequency. Secondly, the natural frequency will increase such that the tuning of the hair across different lengths will change. The question then arises as to the impact of varying S on hair dynamics.

Overall, the results below show that the deflections of cricket cercal hairs are lower than MeD1 spider trichobothria for both electric and aerodynamic stimuli due to the larger magnitude of S from the allometric parameters in Table 1, and the comparatively large damping ratio. Aerodynamically, the results show that the spider hairs are more readily tuned to the biological frequencies over the different lengths for most values of S_m. However, in the cricket system, only increasing S_m produces the same resonant dynamics though with comparatively reduced effect. The changing locations of the minima and ordering of the torque curves for different lengths, S_m and frequency in Figs. 8(a,c,e) and 9(a,c,e) show how the resonant tuning of the hairs varies within the parameter space. Electrostatically, reducing S has a significant, non-linear effect on the deflections of both hair types increasing their magnitudes in each instance highlighting increased sensitivity. These observations are discussed in detail below.

MeD1 spider trichobothria. The effect of varying S on the response of MeD1 spider trichobothria can be illustrated by the maximum hair torque (Fig. 8) the maximum hair deflection (Fig. 8(b,d,f)). Notably, the spider hairs remain in the resonant scheme for each length and value of S_m other than when $S_m < 0.08$ (see Fig. 10(a)).

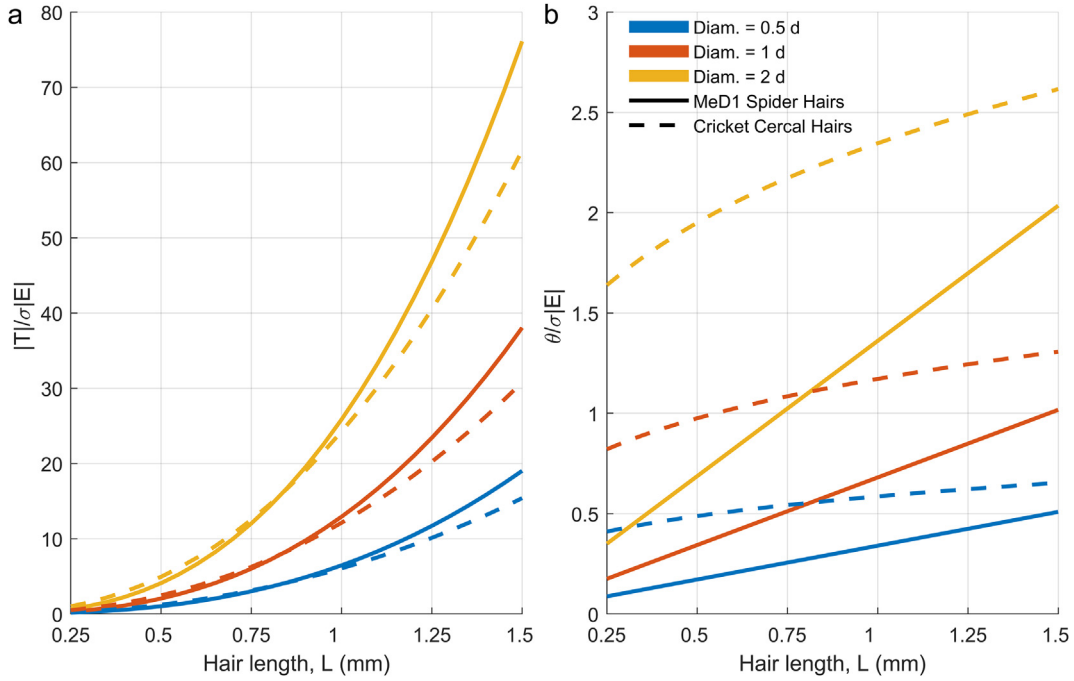

Fig. 7. For MeD1 spider trichobothria and cricket cereal hairs (a) torque per unit $\sigma|E|$ and (b) deflection per unit $\sigma|E|$, as length and diameter vary.

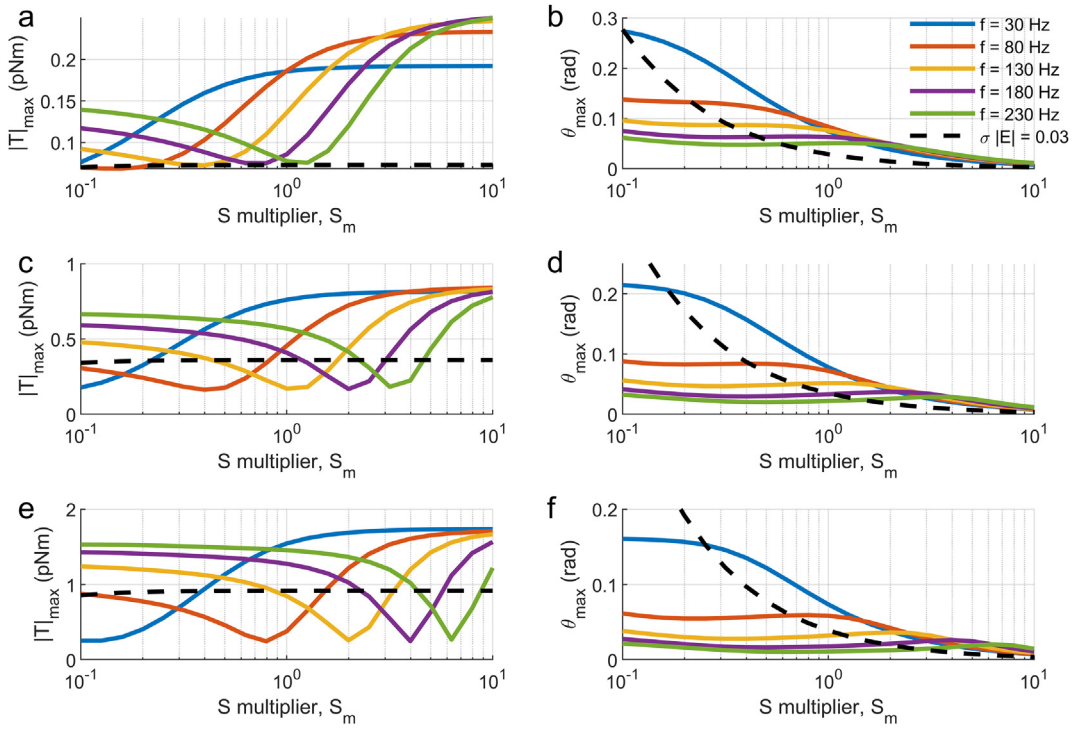

Fig. 8. Varying S for MeD1 spider trichobothria presenting (a,c,e) the maximum torque for hairs of length $L = 0.5, 1.0$ and 1.5 mm respectively, (b, d, f) the maximum deflection, as a function of length and $S \times S_m$ for different frequencies of flow (30 Hz, 80 Hz, 130 Hz, 180 Hz, 230 Hz). The electrostatic response at three different electric interaction strengths is shown: dashed - $\sigma|E| = 0.03\ Nm^{-2}$.

It is immediately apparent that varying S changes the tuning of the hairs across the different lengths. For $S_m < 1$ the hair deflections are reasonably uniform, though distinct, in magnitude for each hair length. Approaching $S_m = O(1)$ the resonant minima across the torque curves initially relates to 30 Hz and changes to higher frequencies as S_m increases and the hairs begin to tune to different biological frequencies. The ordering of the torque curves is also seen to change with the hair tuning. When $S_m = O(10)$ the torque curves converge and become reasonably uniform. The resonant frequency of the hairs is now above the biological range and this behaviour is similar to that seen in Fig. 4 when the hairs detune with length. In raising the resonant frequency outside the biologically relevant range the magnitudes of hair deflection fall rapidly for all lengths.

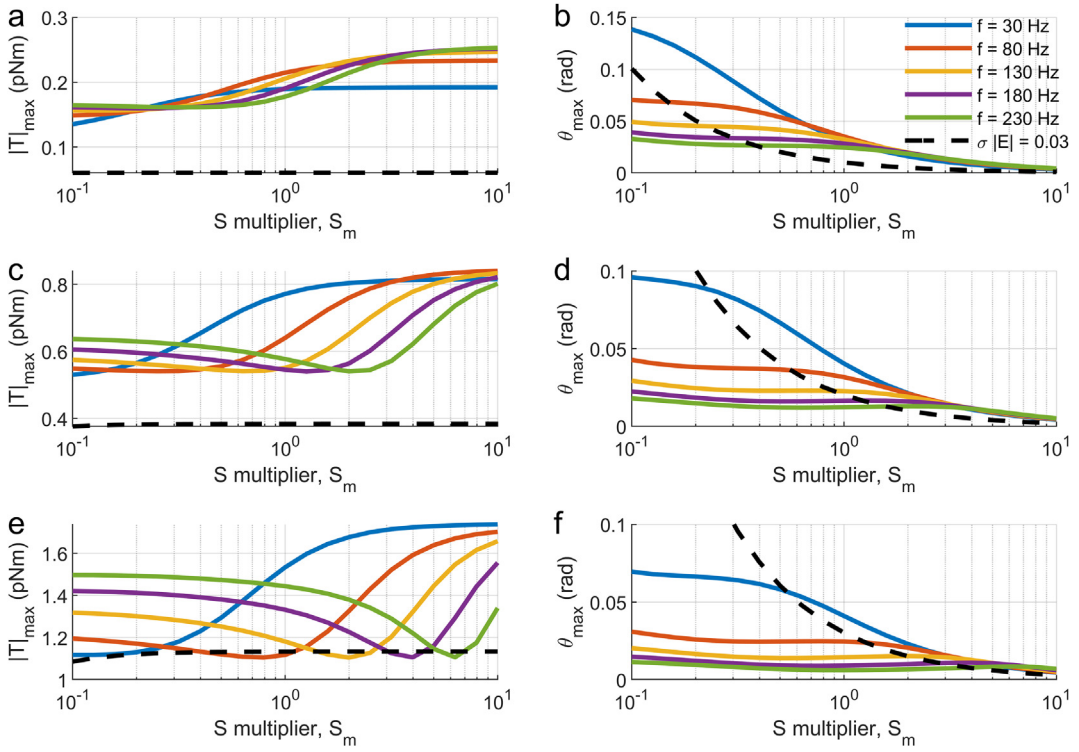

Fig. 9. Varying S for cricket cercal hairs presenting (a,c,e) the maximum torque for hairs of length $L = 0.5, 1.0$ and 1.5 mm respectively, (b, d, f) the maximum deflection, as a function of length and $S \times S_m$ for different frequencies of flow (30 Hz, 80 Hz, 130 Hz, 180 Hz, 230 Hz). The elecrtrostatic response at three different electric interaction strengths is shown: dashed – $\sigma|E| = 0.03\ Nm^{-2}$.

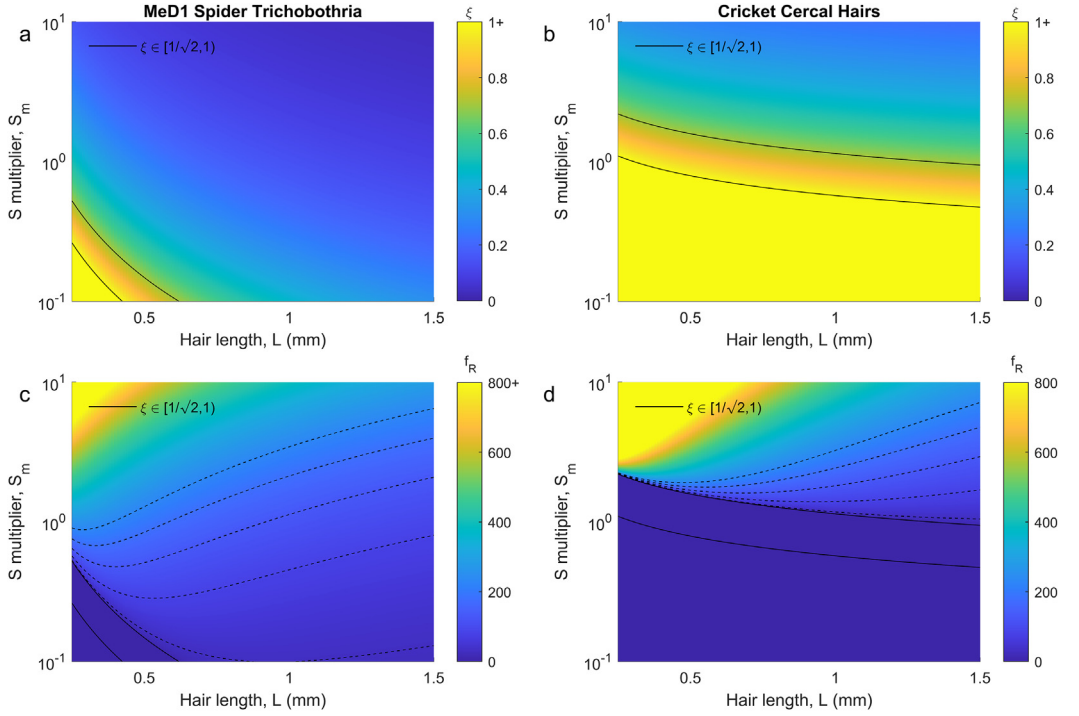

Fig. 10. Phase diagrams for presenting (a,b) the damping ratio, (c,d) the resonant frequency, for MeD1 spider trichobothria (a,c) and cricket cercal hairs (b,d). Each is shown as a function of length and $S \times S_m$. The two solid black lines indicate the region of slight underdamping in which resonance is not possible. The five dashed lines show the relationship between length and S_m for which the respective resonant frequency is 30 Hz, 80 Hz, 130 Hz, 180 Hz and 230 Hz.

Cricket cercal hairs. Fig. 9 shows the effect of varying S on the response of the cricket cercal hairs as measured by the maximum hair torque in panels a,c,e and the maximum hair deflection in panels b,d,f.

For $S_m < 1$ the system is generally overdamped for all hair lengths. As a result, the behaviour of both the torque curves Figs. 9(a,c,e) and the deflection curves Figs. 9(b,d,f) are reasonably uniform in this region of the parameter space. As S_m increases the

hairs become resonantly damped, as first seen in the $L = 1.5mm$ hairs. Yet, overall the effect of resonance is reasonably mild especially for the shorter hairs. This is due to the narrow envelope of resonant frequencies and the damping ratio remaining near $1/\sqrt{2}$ for the biological tuning (this is seen in Fig. 10d) and further explained later).

Similar qualitative behaviours as in the spider system are seen in the torques and deflections showing the resonant tuning of the hairs to the biological frequencies (seen by the moving maxima and minima in Figs. 9(a,c,e)). When $S_m = O(10)$ the torque curves converge as before and the angle of deflection diminishes greatly. This is due to S increasing tenfold and becoming dominant in the equation of motion (1) when compared with R and I.

Electrostatic sensitivity. Regarding the electric response of the hairs in both Figs. 8 and 9, for smaller S_m the hair deflections grow significantly, and diminish with larger S_m. Furthermore, the hair response increases linearly with $\sigma|E|$ and the electrostatic deflection increases with length due to the increased surface charge as previously discussed.

The relationship between hair response and varying S is due to how the steady stimulus effects the hair motion where the dynamics are governed by the relation: $S\theta = \tau$. Since the value of the electrostatic τ is reasonably uniform as S varies in Figs. 8(a,c,e) and 9(a, c,e), a smaller S produces a larger deflection angle whilst larger S reduces the deflection.

The increased deflection with smaller S indicates an increased sensitivity of the hair in response to electrical fields. For smaller S, hairs may produce the same magnitude of response (in comparison to hairs with larger values of S) in response to smaller values of $\sigma|E|$. This indicates that if two such hairs have the same charge (q), the one with a smaller S can detect electrical fields with smaller $|E|$. Similarly, the inverse is true, whereby hairs with smaller S can detect a given electrical stimulus to the same degree deflection with a comparatively lower surface charge.

4.3. Parameter space for the restoring coefficient, S

To understand the impact of varying S more generally we present phase diagrams of the S and L parameter space. The parameter S is varied by some multiplier $S_m \in [0.1, 10]$ and we are interested in understanding how the damping ratio and resonant frequency of each system changes with S and length, and therefore how the expected dynamics vary within the parameter space. All other parameters are kept the same as the correlations in Table 1. Thus, we seek to explore regions of the parameter space where the combination of the oscillator parameters leads to a tuning of the hair, a preference towards aerodynamic sensing and a preference to electrostatic sensing.

In Fig. 10, four different phases planes are presented, two for the MeD1 spider trichobothria and two for the cricket cercal hairs. Firstly, plots in panels a and b show the damping ratio for varying L and $S \times S_m$ for the MeD1 spider trichobothria and the cricket cercal hairs respectively. The colour ranges from yellow-orange-green–blue showing the regions of overdamping (yellow), slight underdamping (orange), resonant underdamping (green) and very resonantly underdamped (blue). The two solid black lines bound the region of slight underdamping and represent the curves along which the combination of S_m and L leads to the critical damping, when $\zeta = 1$, and resonant damping, when $\zeta = 1/\sqrt{2}$.

Secondly, plots in panels c and d show the resonant frequency of the two systems as L and $S \times S_m$ vary. Again, the two solid black curves indicate the region of slight underdamping whilst the five dashed black lines mark the curves along which the combination of S_m and L produce a resonant frequency of 30Hz, 80 Hz, 130 Hz, 180 Hz and 230 Hz respectively. For very small ζ the phase diagram and dashed curves of the resonant frequencies closely resemble those of the natural frequency (not shown) and the parameter space looks very similar.

Overall, the differences between Figs. 10(a,c) (for MeD1 spider trichobothria) and 10(b,d) (for cricket cercal hairs) show why the spider system is more readily tuned to different frequencies as the hair length changes than the cricket system. Namely, in the case of the spider system changing length has a greater effect on the damping ratio and therefore on the resonant frequency such that spider hairs are more distinctly tuned to a wider range of frequencies through changes in length.

In further detail, as shown in the previous analysis, for a well-tuned, resonant aerodynamic response (as in the case of the Med1 spider trichobothria) S_m and L should be such that the magnitude of the natural and resonant frequencies are close to the biological range. In Fig. 10(c,d) this occurs in the regions covered by the dashed lines. As such we expect these regions to represent the "optimal" region for aerodynamic hair tuning to specific biological frequencies since this is where the combination of hair lengths and $S \times S_m$ match the desired frequencies and boundary layer thicknesses. In both plots, the values of S_m that cover this region show that different hair lengths readily tune to different frequencies. Furthermore, the minima of the hair torques for each hair length and frequency in Figs. 8(a,c,e) and 9(a,c,e) coincide with the S_m values and hair lengths along the respective resonant frequency curves.

In the region above the dashed lines both aerodynamic and electrostatic responses are poor. Here the hairs are no longer tuned to the correct frequencies and the damping ratio decreases, narrowing the bandwidth and further diminishing the aerodynamic capability of the hairs in the desired frequency range. Here also, the larger values of S lead to smaller deflections.

Below the dashed lines, the sensitivity of the hairs to electrostatic stimuli begins to improve (as shown in Figs. 8(b,d,f) and 9 (b,d,f)). The aerodynamic deflections do not diminish in this region. The increase in electrostatic sensitivity is a function of smaller S and increased length/hair charge.

Comparing the differences in the cricket cercal hair response and MeD1 spider trichobothria in Figs. 8 and 9, Fig. 10 shows that this is partly due to differences seen in the parameter spaces of the two hairs. In Fig. 10(a) there is a resonant tuning of the MeD1 spider trichobothria over the majority of the parameter space, whereas the cricket cercal hairs in Fig. 10(b) are mainly overdamped or slightly underdamped and damping has a greater influence here. In both cases increasing L or S_m independently decreases the damping ratio. However, in the cricket case changing L has a far smaller impact than in the spider system. This is readily seen in the shape of the solid black curves and colour gradients and explains why a greater variation in hair behaviour is seen in the spider system for different lengths of hairs.

Finally, the four biologically-relevant frequency curves in Fig. 10(d) are closer together than in Fig. 10c) and do not deviate as rapidly from the line solid black line indicating resonant damping. As a result, the damping ratio remains relatively large for the cricket system within the region of biologically relevant resonant tuning. In this region, the bandwidth of the oscillator is broader and covers the range of biological frequencies such that the torque response is less distinct over the different frequencies despite the resonant tuning of the hair. In addition, for the cricket system the orientation of the parameter space is less favourable to variations in the tuning and behaviour of hairs with changing hair length since the gradient of the solid curves and dashed curves are shallower and reasonably uniform with hair length.

4.4. Hair response for varying the damping coefficient, R

Next, we analyse the effect of varying R by a multiplier $R_m \in [0.1, 10]$ through the examination of the hair torques and deflections of three lengths of hair, $L = 0.5, 1.0, 1.5$ *mm*. Increasing the value of R raises the damping ratio, however the natural frequency of the system remains the same. Given the parameters in Table 1, the magnitude of the overall tuning of the hairs will remain within the range of the biological frequencies. Therefore, varying R alters when the system is in the resonant regime, the slightly underdamped or the overdamped regimes, and the fine tuning of the hairs. Hence, the question once again is: What is the overall impact on the hair dynamics as the resonant tuning changes or the hairs become overdamped?

It should be noted that due to the (quasi)-steady assumption of the electrostatic stimulus, varying R will not change the response of the hair within the electrostatic regime. However, curves relating to electrostatic sensing are still included for comparative purpose.

Overall, comparing the two hair systems, both exhibit similar responses to varying R. For small R_m the hair responses are distinct to different frequencies at varying hair lengths. As R increases the hair response becomes less distinct to different frequencies, however the hairs are still fairly reactive until R_m becomes significantly large.

MeD1 spider trichobothria. Fig. 11 shows the effect of varying R by a multiplier $R_m \in [0.1, 10]$ on the hair response of MeD1 spider trichobothria as measured by the maximum hair torque (a,c,e) and the maximum hair deflection (b,d,f). For varying R the system is in the resonant parameter space for most values of R_m other than large values.

For $R_m = O(10^{-1})$ the torque curves for different frequencies are distinctly ordered and vary with hair length. This shows that in the low damping ratio, resonant regime the hairs can be specifically tuned to different frequencies solely by length and thus produce significant hair deflections per unit torque. Furthermore, the torque responses remain reasonably uniform until $R_m = O(1)$ is approached at which the torque curves begin to converge, though the resonant tuning and ordering of the curves remains. This convergence is due to the resonant tuning gradually changing with the increased damping and the hairs having a greater resistance to the airflow. Overall, the resonant effect is less influential as the damping increases.

Finally, as R_m increases further still, the hairs enter the non-resonant, slightly underdamped regime and eventually the overdamped regime for $R_m = O(10)$. The hair response across the frequencies and lengths now becomes reasonably uniform with the torque curves converging further. Additionally, with increasing R_m the hair deflections decrease and also begin to converge, similar to the cricket hair response first seen in Fig. 4. The increased damping and hair resistance are the cause of this effect alongside the loss of resonant tuning.

Cricket cercal hairs. Fig. 12 shows the effect of varying R by a multiplier $R_m \in [0.1, 10]$ on the hair response of cricket cercal hairs as measured by the maximum hair torque (a,c,e) and the maximum hair deflection (b,d,f). Notably the torque responses are of a similar order for both hair types, though the deflections in the cricket system are generally lower due to the higher value of S.

The resonant tuning of hairs to different frequencies with length is seen for small R_m given the ordering of the torque curves. Increasing the value of R eventually causes the cricket system to enter the non-resonant, slightly underdamped regime and overdamped regime for smaller values of R_m than in the spider system. As before, when this occurs the torque increases with greater hair resistance, the deflections diminish and the distinct response of the hairs to different frequencies of flow disappears as the tuning of the hairs is lost.

Electrostatic sensitivity. Regarding the electrostatic response in both cases, since there is no change in the hair behaviour with R the overall conclusions that can be drawn here are limited and only due to the diminishing aerodynamic sensitivity of hairs with R. Most interestingly, the magnitude of the hair response to the

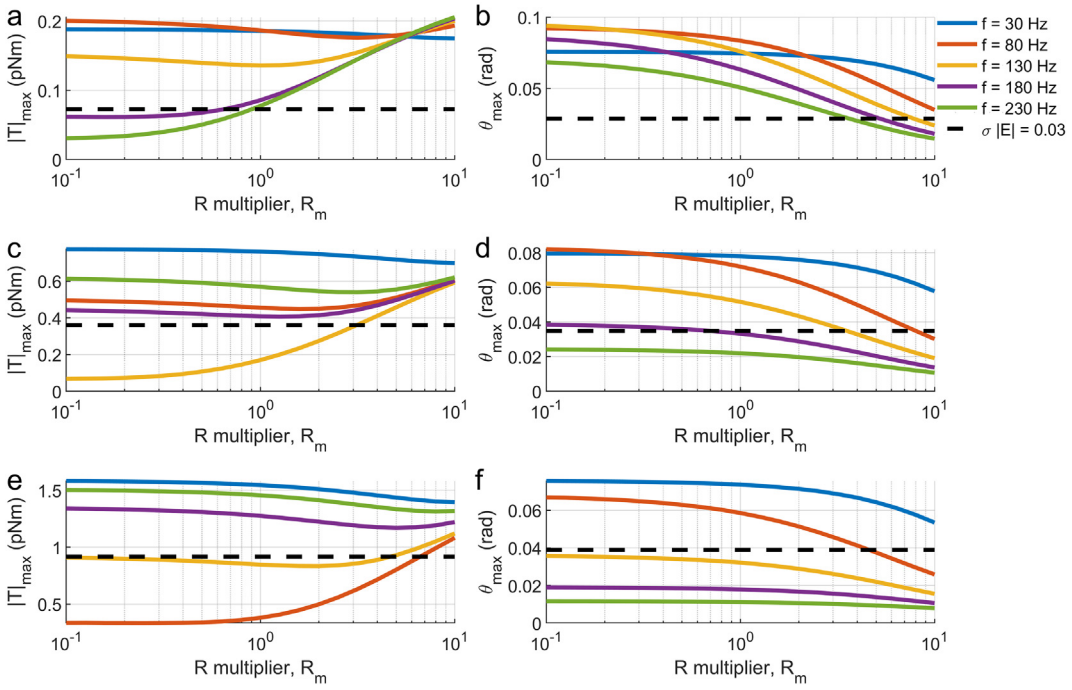

Fig. 11. Varying R for MeD1 spider trichobothria presenting (a,c,e) the maximum torque for hairs of length $L = 0.5, 1.0$ and 1.5 mm respectively, (b, d, f) the maximum deflection, as a function of length and $R \times R_m$ for different frequencies of flow (30 Hz, 80 Hz, 130 Hz, 180 Hz, 230 Hz). The electrostatic response at three different electric interaction strengths is shown: dashed for $\sigma|E| = 0.03\ Nm^{-2}$.

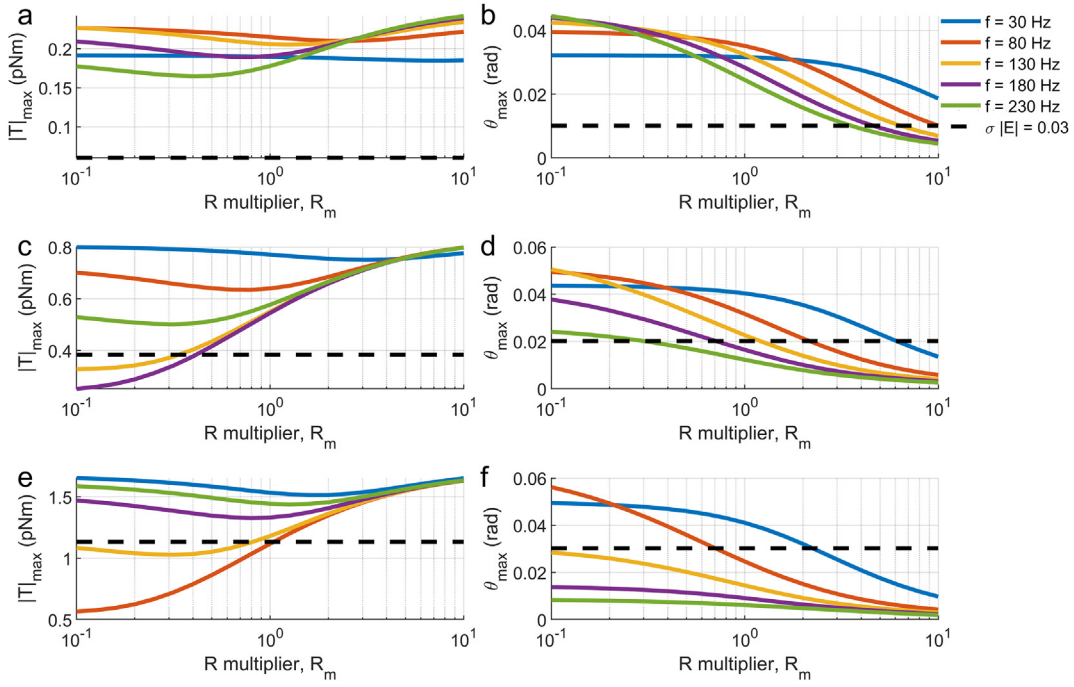

Fig. 12. Varying R for cricket cercal hairs presenting (a,c,e) the maximum torque for hairs of length $L = 0.5, 1.0$ and 1.5 mm respectively, (b, d, f) the maximum deflection, as a function of length and $R \times R_m$ for different frequencies of flow (30 Hz, 80 Hz, 130 Hz, 180 Hz, 230 Hz). The electrostatic response at three different electric interaction strengths is shown: dashed – $\sigma|E| = 0.03\ Nm^{-2}$.

electrostatic stimulus (with regards to torque and angle of deflection) is of a similar order to that of the aerodynamic response for all values of R_m. In addition, this analysis and the previous results indicate that for a slightly underdamped or overdamped system, electrostatics produce comparatively larger deflections than the aerodynamics, especially for longer and thicker hairs. However, this is due to the diminished aerodynamic sensing.

4.5. Parameter space for the damping coefficient, R

To understand the impact of varying R in general we now present phase diagrams for the $R \times R_m$ and L parameter space to show how the damping ratio and resonant frequency of each system changes with R and length, and therefore how the expected dynamics vary within the parameter space.

In Fig. 13 the equivalent four phase diagrams for varying $R \times R_m$ (as in Figs. 10) are presented for MeD1 spider trichobothria and cricket cercal hairs respectively. The two solid black lines again bound the region of slight underdamping and represent the curves along which the combination of R_m and L leads to the critical damping and the resonant damping of the hairs. The five dashed black curves in plots Fig. 13(c) and (d) indicate the curves along which resonant frequencies of 30 Hz, 80 Hz, 130 Hz, 180 Hz and 230 Hz, respectively.

Overall, Fig. 13 shows that hairs can be more readily tuned to different frequencies with hair length in the resonant regime. When the damping ratio is very small, specific resonant frequencies align with specific lengths. As the damping ratio approaches $1/\sqrt{2}$ the parameter space changes such that, rather than the resonant frequency varying only with length (small R_m behaviour), the curves more readily align with specific values of R_m, thus losing their distinct tuning with length.

In detail, the similarity in responses of the spider and cricket systems in Figs. 11 and 12 is understandable given the shape and similarities of the parameter spaces in Figs. 13. The main difference is how the spider's parameter space stretches out more with R_m due to the overall balance with S and I. As such, a larger proportion of the phase diagram in Fig. 13(a) shows a resonant hair response for all lengths in the spider system, whereas for the cricket system in Fig. 13(b) the space is roughly equal in terms of being overdamped or underdamped. Overall, however, the resonant frequency curves in Fig. 13(c) and (d) are geometrically similar and show similar frequency values.

For a well-tuned, resonant aerodynamic response, R_m and L should be such that the magnitude of the resonant frequencies are close to the biological range. Noticeably, the shape of the curves and parameter space here are markedly different to the S_m cases. When the damping ratio is small ($R_m = O(10^{-1})$) there is a clear lack of variation in the resonant frequency with R_m. In this region, hair length has the most significant influence on the hair's resonant tuning with the frequency curves aligning vertically with hair length. This region represents the "optimal" region for hairs of different length to be tuned to specific biological frequencies and boundary layer thicknesses.

As the curve $\zeta = 1/\sqrt{2}$ is approached the resonant frequency curves bend and begin to align with this curve. This significant deformation of the parameter space leads to the loss of frequency tuning with length, particularly in the cricket case (Fig. 13(d)). This indicates more clearly the reason for the diminishing resonant response of the hairs and the convergence of the torque curves in Figs. 11 and 12. That is, for these values of R_m, multiple hair lengths tune to the same frequency and have overlapping bandwidths such that their frequency-distinct responses and the resonant effects diminish. The damping effect is therefore significant here in determining the hair behaviour in terms of the tuning and deflection. Notably, the damping ratio begins to show greater variance with increased hair length here. Whilst the specific tuning is lost, in this region of the parameter space the hairs can still respond with significant deflections to the aerodynamic stimuli in a range that is biologically relevant, as shown by the deflections in the original cricket system (Fig. 4). This is also true when entering into the non-resonant underdamped and overdamped regions. However,

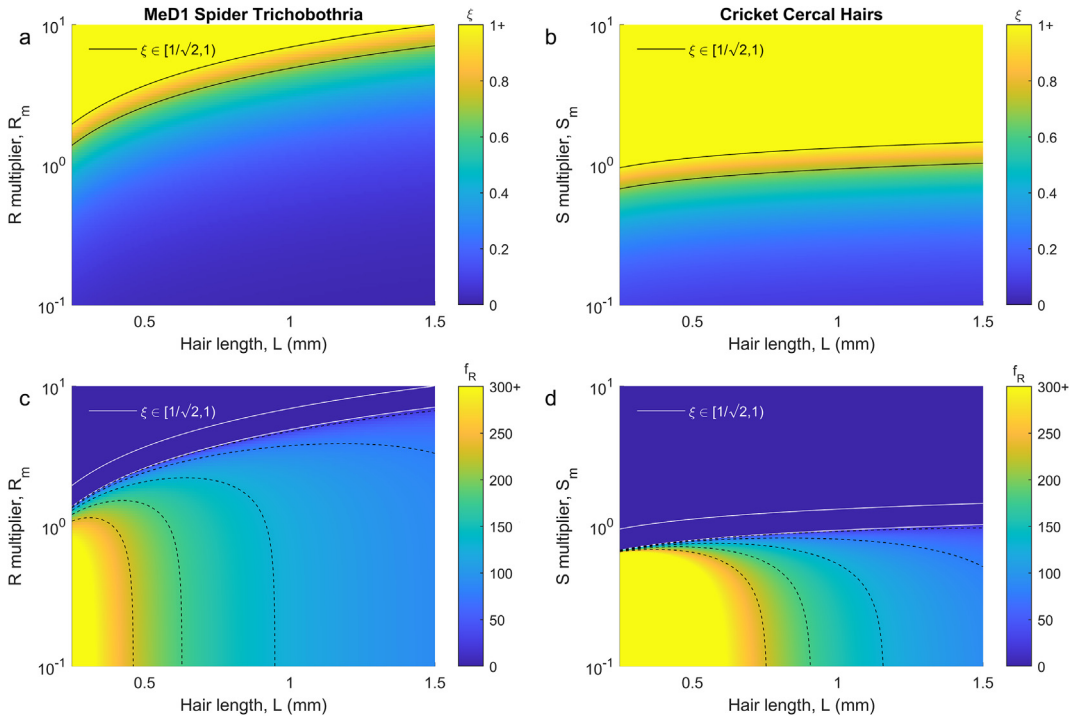

Fig. 13. Phase diagrams for presenting (a,b) the damping ratio, (c,d) the resonant frequency, for MeD1 spider trichobothria (a,c) and cricket cercal hairs (b,d). Each is shown as a function of length and $R \times R_m$. The two solid black lines indicate the region of slight underdamping in which resonance is not possible. The five dashed lines show the relationship between length and R_m for which the respective resonant frequency is 30 Hz, 80 Hz, 130 Hz, 180 Hz and 230 Hz.

if R_m becomes too large and the hairs are significantly overdamped the aerodynamic response diminishes greatly.

5. Bimodality and preferential sensing

Humphrey and Barth, 2007 noted that natural selection has led to hairs having geometries and densities (and thus, I) and cuticular properties and structures (and thus, S and R) such that the natural/resonant frequency and length of mechanosensory hairs matches the frequencies, flow speeds and associated boundary layer thicknesses of aerodynamic sensory importance to the athropod. However, the additional possibility of electrostatic sensing through these hair systems raises important questions such as: What is the parametric feasibility of bimodality? To what extent can these systems be parametrically tuned to favour a given modality?

5.1. Parametric feasibility of bimodality

In Section 3 we examined the mechanical sensitivity of mechanosensory hairs in response to a given stimuli as measured by the maximal induced torque and the maximal hair deflection, c.f. Sections 3.3 and 3.4, Figs. 4 and 6. In addition, to characterise the utility of the hairs in detecting external stimuli, the hair responses were considered with regard to the dynamical properties of the stimulus such as its amplitude steadiness and frequency.

Building upon these ideas, in Section 4 we considered the aerodynamic and electrical sensitivity of the hairs in relation to varying oscillator parameters and stimuli. Aerodynamically, these were measured by the hair's response when driven at/or near the system's resonant frequency and when driven at frequencies outside of the resonant range/when the system lacked resonance, c.f. Figs. 8–13. By comparison, for electrical sensing, strength of stimuli required to produce a similar order of magnitude response as the aerodynamic scenarios was calculated (Figs. 4, 6, 8, 9, 11, 12). As a measure of electrical sensitivity, the torque and deflection per unit $\sigma|E|$ were also calculated (Figs. 5 and 7). These studies help provide an initial basis for understanding the parametric feasibility of bimodality within the shared oscillator space.

To further understand the effect of S and hair geometry on the electrical sensitivity of the system we consider the dependence of $\theta/\sigma|E|$ on $S \times S_m$ and L. This is presented in Fig. 14. Here, the change in electrical sensitivity throughout the parametric domain can be clearly seen with longer hairs and, more influentially, smaller values of S_m increasing the electrical sensitivity of the hair. However, whilst reducing the S parameter further and further seems to pay off with a larger angular sensitivity, past a certain detection threshold, at which a biologically significant deflection occurs and an action potential is emitted, such reductions would become redundant. Overall S determines the scale of electrical field that is detectable given the hair charge. It is therefore best for S to be tuned so that the hairs are sensitive at a length scale that is biologically relevant to the arthropod.

Overlayed on Fig. 14 are five dashed lines that represent the values of S_m that result in the hair being resonantly tuned to either 30, 80, 130, 180 or 230 Hz at each given length (using the allometric parameters I and R given by Table 1). Hence, as in Figs. 10 and 13, resonant tuning within the biologically relevant range occurs for parameter values between and on the dashed lines. As previously noted, the system will have increased frequency-specific sensitivity within these zones. However, as seen from the cricket system in general and in the spider system in Fig. 8, below these lines within the slightly underdamped and overdamped regions biologically significant mechanics are still possible even if the frequency specific response is lost. In Humphrey and Barth, 2007 the sensitivity thresholds of mechanosensory hairs are broadly discussed and it is noted that sensitivity displacement thresholds as small as $0.1^\circ \approx 0.0017$ rad have been recorded for spider trichobothria (Barth and Holler, 1999a). Thus, within this general bound of arthropod sensitivity, hairs tuned between and slightly

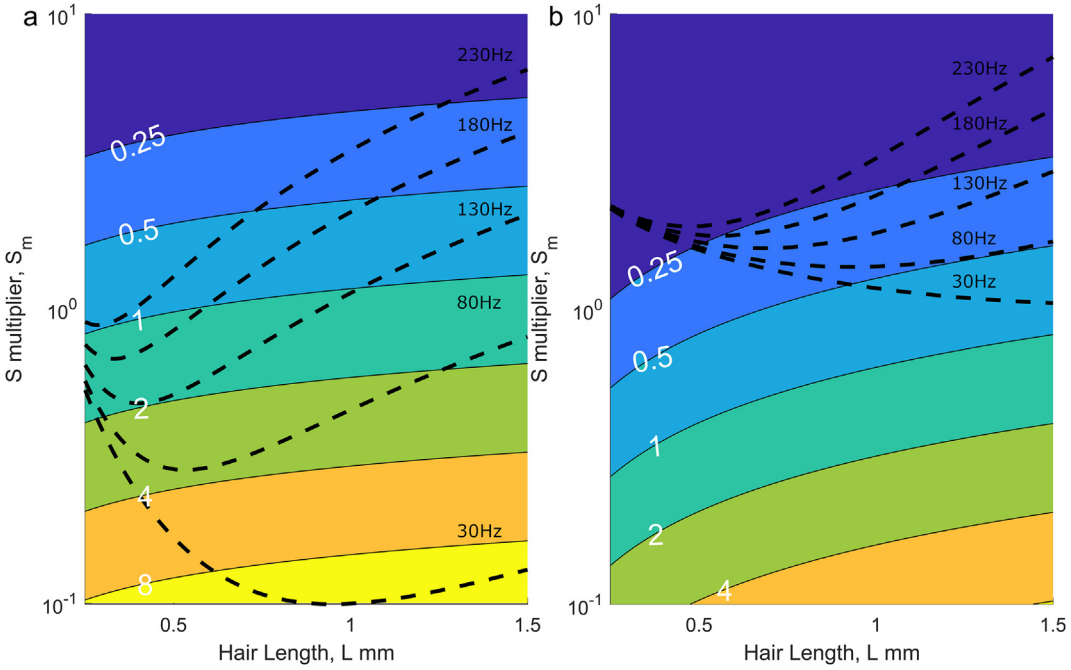

Fig. 14. a) MeD1 spider trichobothria, b) cricket cercal hairs. Contour plot indicating the electric sensitivity of the hair as measured by $\theta/\sigma|E|$ for varying hair length and $S \times S_m$. The five dashed lines show the relationship between length and S_m for which the resonant frequency is 30 Hz, 80 Hz, 130 Hz, 180 Hz and 230 Hz.

below the dashed lines in Fig. 14 may be considered to be aerodynamically sensitive.

5.2. Parametric tuning to favour a given modality

Altogether, seeking to understand the parametric feasibility of bimodality in a single hair system, Fig. 14 uncovers the regions of the parameter space where aerodynamic and electrical sensing are both feasible, and the parametric limitations of the system in detecting each modality. For bimodal operation, S must be low enough for the hair to be electrically sensitive at the correct scale, yet still within the suitable acoustic region of the parameter space (within or just below the dashed line region). For electrical specificity S may be reduced further to increase the electrical sensitivity of the system. Given the logarithmic scaling of the sensitivity contours and S_m, for a single value of S_m it can be seen that hairs of length $L = 1.5\ mm$ can be around twice as electrically sensitive as hairs of length $L = 0.25\ mm$.

For aerodynamic specificity, the system will be parameterised within dashed lines for frequency specific responses or just below this region for general aerodynamic sensing. For large values of S_m, above the dashed line region, sensitivity to both electrostatics and aerodynamics greatly reduces as seen in Figs. 8, 9, 11, and 12.

Exploring bimodality further, a deeper relationship between the two sensory modes can be seen in Fig. 14. For MeD1 spider trichobothria (panel a), in the region where hairs may be resonantly tuned to lower frequencies (80 Hz and below), hair sensitivity to the two modalities is strongly coupled. Here, the hair will be sensitive to the desired frequency whilst being highly sensitive to electrostatic stimuli. Conversely, within the limits of the parameter space, hairs that are resonantly tuned to higher frequencies will be less electrically sensitive. Thus, the tuning of the hairs to certain ranges of frequencies may preclude electrical sensitivity, likewise for certain ranges of frequencies increased sensitivity to electrical fields cannot be avoided.

Moving from the general parameter space to the specific cases of spider MeD1 trichobothria and cricket cercal hairs, Fig. 15 presents the dependence of resonant frequency and electrical sensitivity with hair length for the two hairs systems (these results are for the allometric parameters presented in Table 1). The balance between electrical and aerodynamic sensitivity can be clearly seen.

With increasing length both spider and cricket hairs increase in electrical sensitivity. For spiders this is accompanied by a reduction in bandwidth and therefore an increased sensitivity to a thin band of frequencies. Notably, for hair lengths above about 0.9 *mm* and frequencies in the range of about 100–150 Hz the increase in electrical sensitivity is accompanied by only a slight reduction in bandwidth. For cricket hairs there is no such relationship between aerodynamic specificity and electrical sensitivity except for hairs longer than about 1.3 *mm* and then only for frequencies below about 30 Hz.

To this end, the nature of bimodality differs between the spider and cricket systems. In the spider system there is a strong coupling between aerodynamic specificity and electrostatic sensitivity with hair length determining both. Thus, increased sensitivity in one modality cannot be uncoupled from increased sensitivity in the other. For cricket hairs however the two modalities are more uncoupled. Here, hair length can be more freely varied with little effect on the aerodynamic sensitivity, yet with a significant impact on electrostatic sensitivity. Thus, across hair lengths the aerodynamic response is more equitable, whilst the electrostatic sensitivity varies widely.

5.3. Other considerations

The results above point to the region in parameter where the system is resonant and tuned to lower frequencies, or slightly underdamped systems as possessing, as being the most appropriate for bimodality. However, there are further considerations to be made to understand better the balance of hair tuning to both modalities such as the temporal dynamics for a moving source of the stimulus. For example, the low attenuation rate of a resonant system is likely to hinder the temporal resolution of the sensory system. A moving sound or electric source may thus generate a rate of change of the stimulus that is larger than the integration time of the sensory system. This putative process constitutes a constraint

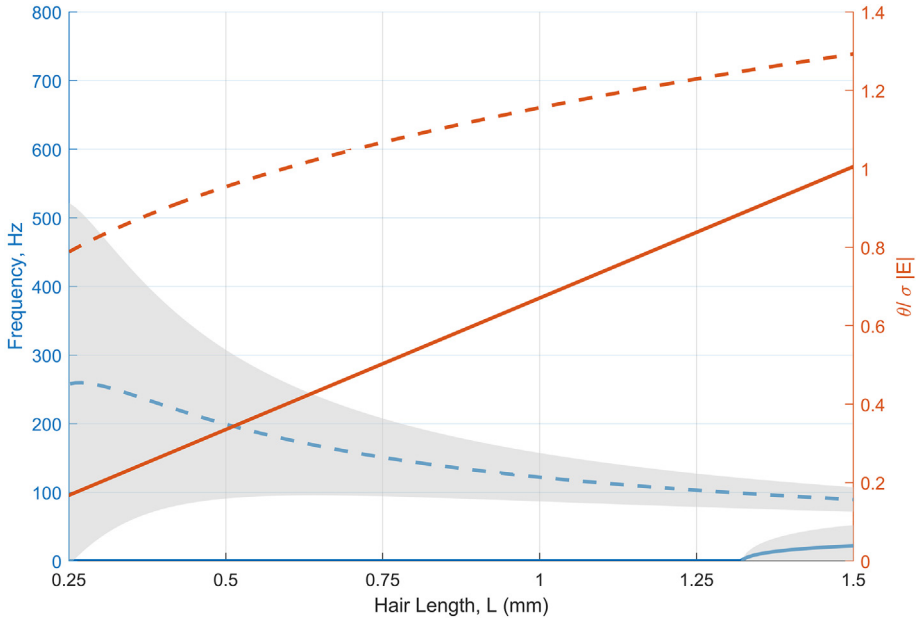

Fig. 15. Resonant frequency with bandwidths and electrostatic sensitivity versus hair length for the allometric parameters in Table 1. Solid lines – cricket cercal hairs, dashed lines – spider MeD1 trichobothria.

on any sensory process and its dynamic response. Mechanosensory hairs certainly are the product of such constraint, should they be part of a directionally sensitive system. Consequently, when the damping ratio is too small where S_m is large, the hair disturbance will last for a longer time and potentially inhibit the sensing of subsequent disturbances. In addition, attenuation rate will be higher in the non-resonant system, where S_m is small, such that for a passing signal the hair response will fade more quickly and be available for a future signal. This type of response enhances the capacity for high temporal resolution in the detection of dynamic signals and the capacity to discriminate signal from noise.

6. Discussion and conclusions

We have analysed the motion of two different and well-known biological mechanosensory systems, the MeD1 spider trichobothria and the cricket cercal hair, offering a systematic appraisal of the physics of mechanosensory hair motion. We have shown that the physical response of these systems varies greatly both in the detection of aerodynamic and electrostatic stimuli. This is due to the two systems possessing distinctly different oscillator parameters, S, R, I, as defined by hair geometry and cuticular properties.

By comparing and contrasting the wider parameter spaces in which the hairs exist, we have also shown how varying S, R or I can gradually alter the hair behaviour until the mechanics of the system change completely. Under the aerodynamic stimulus, the most significant changes occur when moving between resonant and non-resonant regions in the parameter space. Under the electrostatic stimulus, the hair, diameter and spring constant S have the largest effect on the hair response due to their influence on the hair charge and Coulomb interaction.

Aerodynamically, we have shown that, on the one hand, small perturbations of these oscillator parameters may not have a significant effect on the dynamics or the tuning of hairs to biological stimuli so long as the parameters remain within the relevant region of the parameter space. On the other hand, larger changes in these parameters may result in resonant tuning outside of the biologically relevant range, a loss of resonant tuning altogether, or overall diminished aerodynamic sensitivity. We have also shown the underlying features of the parameter spaces for S and hair length, and R and hair length, and the relative influence of each parameter on the hair behaviour in these spaces. With I fixed by the hair geometry and density of the hair, varying S relative to I sets the magnitude of the natural frequency and generally the range of frequencies that the hair may match to. Whilst varying R, relative to S and I, determines more specifically whether the hair is in the resonant space and how the hair tunes with length.

For the resonant regime, since the motion of hairs of a given length will closely match a specific flow frequency, an array of appropriately tuned resonant hairs of mixed lengths is thus capable of readily detecting and discerning different frequencies and, depending on the organisation of the hairs, the location of the source. In contrast, whilst in the slightly underdamped or overdamped systems there is less discrimination between low frequencies, such hairs may respond somewhat equally to a wider range of driving frequencies (Theunissen et al., 1996). Here, discrimination may then take place using ensembles of spatially-distributed and differently tuned sensory hairs and associated primary neurones, as seen in bushcricket hearing (Montealegre-Z et al., 2012), yielding a range of responses that together span the biologically relevant bandwidth (Steinmann and Casas, 2017; Theunissen et al., 1996).

With respect to the electrostatic response of hairs, we found that for improved quasi-static electric sensing S should be small and the hair should be longer and/or thicker. Typically, adjustment of S and diameter is governed by hair length and/or varying cuticular properties, yet, a careful balance is to be struck. While S increases with hair length, so does the hair's charge through the change in length and diameter. Depending on the system, this charge increase can outweigh the increased value of S. For example, re-writing the allometric parameters for diameter and S in Table 1 in terms of $\hat{L}$ $mm = O(1)$:

Parameter	Cricket cercal hair (Shimozawa et al., 1998)	Spider MeD1 trichobothria (Humphrey and Barth, 2007)
$d\ m$	$8.1502 \times 10^{-6}\hat{L}^{0.67}$	$7.6453 \times 10^{-6}\hat{L}^{0.3063}$
$S\ kgm^2s^{-2}$	$1.9 \times 10^{-11}\hat{L}^{1.67}$	$1.0339 \times 10^{-11}\hat{L}^{2.030}$

it can be seen that the diameter of the hair is of a larger order of magnitude than S and hence changes in diameter with length will have a greater influence on the system. Indeed, since both S and the hair diameter vary greatly with length, hair length becomes a significant differentiator in electrostatic sensitivity, as shown in the cricket system. Notably, this is an important observation for the manufacture and design of bio-inspired micro-electromechanical systems that may utilise electrostatic mechanosensors. In particular, large variations in the diameter of hairs that are the same length are unlikely in biological systems, however in manufactured systems varying the diameter of the hairs individually or within an array is more feasible and as such the electrostatic benefits of these variations may be readily used.

The present analyses altogether point to the presence of a delicate balance and fine tuning between the oscillator's parameters in determining possible bimodality in the system. Importantly, within the range of biological parameters considered it has been shown that it is feasible for charged mechansensory hairs to detect electrostatic stimuli to a similar degree as aerodynamic stimuli. Thus, bimodality is possible within the considered parameter space and hair tuning. Futhermore, our analysis has shown how the parameterisation or geometry of hair system with a single morphological design may lead to the preferential sensing of either modality, the possible sensing of both modalities, and the limit at which the hair is unable to reasonably detect either.

For instance, in the setting of S, too high of a value leads to a tuning of the hairs far above desired frequencies and the deflection is inhibited in response to both electrical and aerodynamic stimuli. For smaller S there are benefits regarding quasi-static electric sensing however the aerodynamic hair tuning may fall below the range of biologically-relevant frequencies, and the hair departs from sensitive resonant behaviour. As previously noted, electrostatically, there is a natural threshold to how far S may be reduced. Whilst the hair may gain sensitivity to smaller stimuli, if the hair becomes too sensitive it will be unable to distinguish electrostatic signals from electrostatic noise or will be unable to resolve electrostatic stimuli at the correct length scales. As for the setting of R, the smaller the value relative to S and I, the smaller the damping ratio becomes, setting the hairs within the resonant regime. However, with this arrangement, the attenuation rate decreases making the system slower to return to steady state after signal offset. For R too high, the damping ratio will be large such that the system is no longer resonant and can even become overdamped such that hair resistance becomes significant, driving the system to return to steady state without oscillation. In effect, there is a natural mechanical and sensory limit to the relative adjustment and balance between S and R for the mechanosensory hair to fulfil its biological function in response to either modality in turn, or indeed for bimodal sensing.

Accordingly, we hypothesise the existence of two types of mechanosensory hair systems endowed with electrostatic reception. The first system consists of general electrostatic sensors and specific aerodynamic sensors. Such a system may resemble the resonant spider system in which the two stimuli can elicit a similar magnitudes of hair response in terms of torque and deflection across lengths. Essentially, hair length leads to a change in aerodynamic tuning, whilst length does not have as significant a role in electrostatic sensitivity. Thus, the two stimuli have different effects and roles in one single system. Whilst it is known that dynamic sound signals will trigger hairs of different lengths depending on the frequency, location and movement of the stimulus, electrostatic actuation is poised to provide a quasi-steady perturbation that aides location detection by deflecting the hairs simultaneously. At this point, the exact interplay between these distinct stimuli in naturally occurring situation remains unknown.

The second system consists of specific electrostatic sensors and general aerodynamic sensors. This sensor type is proposed to resemble the cricket system and present the balance of the oscillator parameters with length seen there. For this system the electrostatic response is significantly stronger for longer hairs, whilst the aerodynamic sensitivity diminishes quickly with length. In such cases, shorter hairs may provide aerodynamic sensing since there is little differentiation in the hair behaviour with length and frequency flow, whilst longer hairs are more dedicated to electrostatic sensing.

It is worth noting that there are two main limitations of the analysis presented here. Firstly, the metrics used to evaluate the systems were the maximum hair torque and hair deflection only. When aerodynamics are considered, these metrics only provides a snapshot of a dynamic process. Since some of the benefits and drawbacks of the resonant versus non-resonant systems can be further revealed using a dynamic context, $\dot{\theta}$ and $\ddot{\theta}$ could also be considered. Secondly, our discussion of source location is confined to the static cases, whilst in reality, either through the movement of the source or the receiver, stimuli will change in space and time. The temporal aspects of mechanosensory systems have recently gained more attention within the literature with several key studies describing such dynamics in great detail (Casas et al., 2008; Casas and Steinmann, 2014; Steinmann and Casas, 2017). As shown by these studies, temporal dynamics have a non-negligible effect on the dynamics of the hair motion, especially when carrying out sensory information transformation and transfer in considerations of the two bimodal regimes. In regard of the above, a comparison of the dynamic responses of the overdamped cricket cercal hairs and resonantly damped spider trichobothria in response to aerodynamic impulses was carried out in Kant and Humphrey, 2009, and later in Casas et al., 2008; Casas and Steinmann, 2014; Steinmann and Casas, 2017 where particular attention was paid to cricket hair systems and further insights gained from those presented in Kant and Humphrey, 2009 (including some corrections). Understanding the hair aerodynamic response also serves to highlight that a large number of questions remain as to the effects of the parametric tuning in the context of electroreception and electrodynamic stimuli presentation.

Altogether, the results presented here highlight the importance of understanding both the parameter spaces and response envelopes of mechanosensory hairs, in terms of their viscous coupling to the atmospheric environment and their Coulomb interaction with ambient electric fields. In light of this approach, more empirical evidence is needed to characterise a sensory system so prevalent and that underpins the lives of arthropods. In particular, as sensory hairs are rarely found alone, it will be paramount to study the impact of differently-tuned hairs within an array. A key question is whether and how multiple hairs working together attain emergent sensory properties beyond the capacity of single, independent hairs. Further, what role does electrostatic and aerodynamic coupling play in information acquisition for such spatially-distributed sensory systems? Enticingly, questions remain outstanding as to whether and how hair arrays extract information about source location and velocity.

Funding

This work was supported by BBSRC (BB/T003235/1) to DR and IVC, and an ERC AdG grant ElectroBee to DR.

CRediT authorship contribution statement

Ryan A Palmer: Methodology, Formal analysis, Writing - original draft. **Isaac V Chenchiah:** Conceptualization, Writing - review & editing. **Daniel Robert:** Conceptualization, Writing - review & editing, Supervision, Funding acquisition.

Declaration of Competing Interest

The authors declare that they have no known competing financial interests or personal relationships that could have appeared to influence the work reported in this paper.

Acknowledgements

We thank Dr. B Cummins for helpful conversations and making available the base code for the fluid-hair analysis.

References

Amador, G.J., Matherne, M., Waller, D.A., Mathews, M., Gorb, S.N., Hu, D.L., 2017. Honey bee hairs and pollenkitt are essential for pollen capture and removal. Bioinspiration & Biomimetics 12, (2) 026015.

Barth, F.G., 2004. Spider mechanoreceptors. Current Opinion in Neurobiology 14 (4), 415–422.

Barth, F.G., Höller, A., 1999a. Dynamics of arthropod filiform hairs. V. The response of spider trichobothria to natural stimuli. Philosophical Transactions of the Royal Society of London. Series B: Biological Sciences 354 (1380), 183–192.

Barth, F.G., Höller, A., 1999b. Dynamics of arthropod filiform hairs. V. The response of spider trichobothria to natural stimuli. Philosophical Transactions of the Royal Society of London. Series B: Biological Sciences 354 (1380), 183–192.

Barth, F.G., Wastl, U., Humphrey, J.A., Devarakonda, R., 1993. Dynamics of arthropod filiform hairs. II. Mechanical properties of spider trichobothria (*Cupiennius salei* Keys.). Philosophical Transactions of the Royal Society of London. Series B: Biological Sciences 340 (1294), 445–461.

Barth, F.G., Humphrey, J.A., Wastl, U., Halbritter, J., Brittinger, W., 1995. Dynamics of arthropod filiform hairs. III. Flow patterns related to air movement detection in a spider (*Cupiennius salei* Keys.). Philosophical Transactions of the Royal Society of London. Series B: Biological Sciences 347 (1322), 397–412.

Bathellier, B., Barth, F.G., Albert, J.T., Humphrey, J.A., 2005. Viscosity-mediated motion coupling between pairs of trichobothria on the leg of the spider *Cupiennius salei*. Journal of Comparative Physiology A 191 (8), 733–746.

Callahan, P.S., 1975. Insect antennae with special reference to the mechanism of scent detection and the evolution of the sensilla. International Journal of Insect Morphology and Embryology 4 (5), 381–430.

Casas, J., Dangles, O., 2010. Physical ecology of fluid flow sensing in arthropods. Annual Review of Entomology 7 (55), 505–520.

Casas, J., Steinmann, T., 2014. Predator-induced flow disturbances alert prey, from the onset of an attack. Proceedings of the Royal Society B: Biological Sciences 281 (1790). 20141083.

Casas, J., Steinmann, T., Dangles, O., 2008. The aerodynamic signature of running spiders. PLoS One 3, (5) e2116.

Clarke, D., Whitney, H., Sutton, G., Robert, D., 2013. Detection and learning of floral electric fields by bumblebees. Science 340 (6128), 66–69.

Clarke, D., Morley, E., Robert, D., 2017. The bee, the flower, and the electric field: electric ecology and aerial electroreception. Journal of Comparative Physiology A 203 (9), 737–748.

Cortez, R., 2001. The method of regularized Stokeslets. SIAM Journal on Scientific Computing 23 (4), 1204–1225.

Cummins B., Gedeon T.S., 2007. A refined model of viscous coupling between filiform hairs in the cricket cercal system. In: ASME International Mechanical Engineering Congress and Exposition 2007 Jan 1 (vol. 43025, pp. 1301–1309)..

Cummins, B., Gedeon, T., Klapper, I., Cortez, R., 2007. Interaction between arthropod filiform hairs in a fluid environment. Journal of Theoretical Biology 247 (2), 266–280.

Erickson Jr, E.H., 1982. Evidence for electrostatic enhancement of odor receptor function by worker honeybee antennae. Bioelectromagnetics: Journal of the Bioelectromagnetics Society, The Society for Physical Regulation in Biology and Medicine, 3. The European Bioelectromagnetics Association, pp. 413–420.

French, A.P., 2003. Vibrations and Waves, The MIT Introductory Physics Series. W. W. Norton and Co., New York.

Humphrey J.A., Barth F.G., 2007. Medium flow-sensing hairs: biomechanics and models. Advances in Insect Physiology. 2007;34:1-80..

Humphrey, J.A., Devarakonda, R., Iglesias, I., Barth, F.G., 1993. Dynamics of arthropod filiform hairs. I. Mathematical modelling of the hair and air motions. Philosophical Transactions of the Royal Society of London. Series B: Biological Sciences 340 (1294), 423–444.

Jacobs, G.A., 1995. Detection and analysis of air currents by crickets. BioScience 45 (11), 776–785.

Kant, R., Humphrey, J.A., 2009. Response of cricket and spider motion-sensing hairs to airflow pulsations. Journal of The Royal Society Interface 6 (40), 1047–1064.

Koh, K., Robert, D., 2020. Bumblebee hairs as electric and air motion sensors: theoretical analysis of an isolated hair. Journal of the Royal Society Interface 17 (168), 20200146.

Kumagai, T., Shimozawa, T., Baba, Y., 1998a. Mobilities of the cercal wind-receptor hairs of the cricket, *Gryllus bimaculatus*. Journal of Comparative Physiology A 183 (1), 7–21.

Kumagai, T., Shimozawa, T., Baba, Y., 1998b. The shape of wind-receptor hairs of cricket and cockroach. Journal of Comparative Physiology A 183 (2), 187–192.

Landolfa, M.A., Miller, J.P., 1995. Stimulus-response properties of cricket cereal filiform receptors. Journal of Comparative Physiology A 177 (6), 749–757.

Magal, C., Dangles, O., Caparroy, P., Casas, J., 2006. Hair canopy of cricket sensory system tuned to predator signals. Journal of Theoretical Biology 241 (3), 459–466.

Montealegre-Z, F., Jonsson, T., Robson-Brown, K.A., Postles, M., Robert, D., 2012. Convergent evolution between insect and mammalian audition. Science 338 (6109), 968–971.

Morley, E.L., Robert, D., 2018. Electric fields elicit ballooning in spiders. Current Biology 28 (14), 2324–2330.

Shimozawa, T., Kanou, M., 1984. Varieties of filiform hairs: range fractionation by sensory afferents and cereal interneurons of a cricket. Journal of Comparative Physiology A 155 (4), 485–493.

Shimozawa, T., Kumagai, T., Baba, Y., 1998. Structural scaling and functional design of the cercal wind-receptor hairs of cricket. Journal of Comparative Physiology A 183 (2), 171–186.

Shimozawa, T., Murakami, J., Kumagai, T., 2003. Cricket wind receptors: thermal noise for the highest sensitivity known. InSensors and Sensing in Biology and Engineering 2003 (pp. 145–157). Springer, Vienna..

Southwick, E.E., 1985. Bee hair structure and the effect of hair on metabolism at low temperature. Journal of Apicultural Research 24 (3), 144–149.

Southwick, E.E., Heldmaier, G., 1987. Temperature control in honey bee colonies. Bioscience 37 (6). 395-9.

Steinmann, T., Casas, J., 2017. The morphological heterogeneity of cricket flow-sensing hairs conveys the complex flow signature of predator attacks. Journal of The Royal Society Interface 14 (131), 20170324.

Sutton, G.P., Clarke, D., Morley, E.L., Robert, D., 2016. Mechanosensory hairs in bumblebees (*Bombus terrestris*) detect weak electric fields. Proceedings of the National Academy of Sciences 113 (26). 7261-5.

Tautz, J., 1979. Reception of particle oscillation in a medium–an unorthodox sensory capacity. Naturwissenschaften 66 (9), 452–461.

Tautz, J., Markl, H., 1978. Caterpillars detect flying wasps by hairs sensitive to airborne vibration. Behavioral Ecology and Sociobiology 4 (1), 101–110.

Taylor, J.R., 2005. Classical Mechanics. University Science Books.

Theunissen, F.R., Roddey, J.C., Stufflebeam, S.T., Clague, H.E., Miller, J.P., 1996. Information theoretic analysis of dynamical encoding by four identified primary sensory interneurons in the cricket cercal system. Journal of Neurophysiology 75 (4), 1345–1364.

Thurm U., 1965. An Insect Mechanoreceptor Part I: Fine Structure and Adequate Stimulus. InCold Spring Harbor Symposia on Quantitative Biology 1965 Jan 1 (vol. 30, pp. 75–82). Cold Spring Harbor Laboratory Press..

Thurm, U., 1965 An insect mechanoreceptor part II: Receptor potentials. InCold Spring Harbor symposia on quantitative biology 1965 Jan 1 (vol. 30, pp. 83–94). Cold Spring Harbor Laboratory Press..